REMOTE SENSING FOR ASSESSING WETLAND - GROUNDWATER INTERACTION IN THE KOGELBERG BIOSPHERE RESERVE

JEANINE ENGELBRECHT

Thesis presented in partial fulfilment of the requirements for the degree of Master of Natural Sciences at the University of Stellenbosch.

Supervisor: Prof. HL Zietsman

Co-supervisor: Dr. K Riemann

December 2005

Department of Geography and Environmental studies

DECLARATION

I, the undersigned, hereby declare that the work contained in this thesis is my own original work and that I have not previously in its entirety or in part submitted it at any university for a degree.

ABSTRACT

The Table Mountain Group (TMG) Aquifer System is a regional fractured aquifer system with a large potential as a source of future water supplies in the Western and Eastern Cape. This system is currently under consideration for large-scale water abstraction. Many terrestrial ecosystems, however, are dependent on these groundwater resources for survival. Exploitation of ground water resources at a rate exceeding the rate of natural recharge would result in a lowering of the water table and the drying up of seeps.

The main objective of this study was to determine if satellite remote sensing data can be used for the detection of groundwater-dependent wetlands, and secondly, to use multi-temporal imagery for estimating seasonal changes experienced in wetland communities in relation to surrounding vegetation. The Kogelberg Biosphere Reserve, situated approximately 30km to the east of Cape Point in the Western Cape, South Africa, was selected for investigation. To accomplish the objectives, three Landsat 7 ETM+ images (path/row: 175/84) captured on 22 September 2001, 18 May 2002 and 23 September 2002 were acquired. Image fusion of the multispectral bands (30m resolution) with the panchromatic band (15m resolution) provided 15m multispectral images for analysis purposes. Geometric correction, radiometric normalisation and atmospheric corrections was performed in order to ensure pixel-level comparability between images. Once comparability between images was guaranteed, vegetation indices and tasselled cap components were derived to provide threshold values of moisture stress indicators and productivity estimations of wetland communities in relation to surrounding non-wetland communities. Additionally, change vector analysis on these transformations provided the ability to detect and assess the seasonal changes experienced by these communities during an annual cycle. The results of these transformations were combined in a rule-based image classifier in order to assist in estimating the seasonal dependency of observed wetland communities.

The ability to use Landsat 7 images and the abovementioned image processing procedures to identify wetland communities with a high probability of groundwater interaction was demonstrated with a high degree of accuracy (78%). It is recommended that future studies concentrate on increasing classification accuracies, while focusing on incorporating these techniques into a remote monitoring system for assessing the impacts of groundwater extraction on the groundwater-dependent wetland communities.

OPSOMMING

Die Tafelberg Groep (TBG) Akwifer is 'n regionale verskuiwingsakwifer sisteem met groot potensiaal as toekomstige waterbron vir die Wes- en Oos-Kaap. Grootskaalse grondwater-onttrekking uit hierdie sisteem word tans ondersoek. Baie terrestriële ekosisteme is egter vir oorlewing van grondwaterbronne afhanklik. Grondwaterontginning teen 'n tempo hoër as die natuurlike aanvultempo sal die watertafel laat daal en syfersones laat opdroog.

Die hoofdoel van die studie was om te bepaal of satellietbeelde gebruik kan word om grondwater-afhanklike vleilande waar te neem, en om 'n tydsreeks van beelde te gebruik om die seisoenale verandering in vleilandgemeenskappe relatief tot omliggende plantegroei te raam. Die Kogelberg Biosfeer Reservaat, ongeveer 30km oos van Kaappunt, is as studiegebied geïdentifiseer. Drie Landsat 7 beelde (baan/ry: 175/84) van 22 September 2001, 18 Mei 2002 en 23 September 2002 is ontleed. Die Landsat 7 multispektrale bande (30m resolusie) is met behulp van beeld-fusietegnieke met die panchromatiese band (15m resolusie) gekombineer om multispektrale beelde te lewer met 15m grondresolusie. Geometriese korreksie, radiometriese normalisering en atmosferiese korreksie is op elk van die beelde toegepas om beeld-selvlak vergelykings tussen beelde 'n moontlikheid te maak. Met beeldvergelykbaarheid verseker, is plantegroei-indekse en 'tassled cap' transformasies gebruik om afsnywaardes vir vleiland-identifikasie te bereken. Verder is veranderingsvektor-analises op die transformasies bereken om die seisoenale veranderinge oor die jaarsiklus in vleilande te bepaal. Die resultate hiervan is vervat in 'n reël-gebaseerde beeldklassifiseerder waarmee vleilande se seisoenale grondwater afhanklikheid geraam is.

Die vermoë om vleilande met 'n hoë waarskynlikheid van grondwater interaksie uit Landsat 7 beelde te identifiseer is met 'n hoë vlak van totale akkuraatheid (78%) gedemonstreer. Die aanbeveling is dat toekomstige studies moet fokus op die verhoging van hierdie klassifikasie akkuraathede. Die tegnieke moet toegespits word op die ontwikkeling van 'n afstandswaarnemingstelsel om die impak van grondwater onttrekking op grondwater-afhanklike vleilande te moniteer.

ACKNOWLEDGEMENTS

The author would like to acknowledge the following people or institutions that made the successful completion of this study possible:

- Prof. Zietsman and Dr. Riemann, my supervisors, for their input, support and advice;
- Wolgang Lück for all his advice, especially during the image preprocessing stages of this study. His help is greatly appreciated;
- Mr. Adriaan van Niekerk for his invaluable advice where image classification is concerned;
- Prof. IJ van der Merwe for introducing me to Dr. Charlie Boucher who in turn introduced me to the TMG-Eco project team;
- Christine Colvin and David Le Maitre at the CSIR, Stellenbosch, for giving me the opportunity to work on this project and for offering their collaboration;
- The Department of Geography and Environmental Studies for providing me with a post-graduate bursary for the first year of study;
- To the Satellite Application Centre, especially Elsa de Beer, for providing me with the Landsat 7 imagery needed for this study;
- To the Western Cape Nature Conservation Board, Scientific Services for providing me with the vegetation map of the area of interest;
- Tim Aston who went above and beyond to assist in identifying some groundtruth sites during fieldwork related to his study;
- Prof. Zietsman, Dr. Hennie van der Berg, Dr. Riemann and Mr. van Niekerk for their invaluable input after the first draft was presented;
- Dirk van Zyl for his love, support and providing a shoulder to lean on when the going was tough;
- My mother, without her financial and moral support my student career would not have been possible;
- Special thanks are also in order to the staff of the Department of Geography and Environmental studies for their friendly disposition and support throughout the year.

Thanks to them all and all not mentioned who helped in any way.

CONTENTS

FIGURES

TABLES

CHAPTER 1: BACKGROUND TO THE STUDY

1.1 INTRODUCTION TO THE STUDY

The limited supply of – and the increasing demand for – water, together with the variability of rainfall, makes water resource availability a critical factor for the City of Cape Town (Ninham Shand 2004). As available surface water resources become over-exploited, attention is turning to groundwater as a supplementary source. However, the exploitation of groundwater resources poses unique problems. Many ecosystems are dependent on groundwater resources for survival, especially groundwater-fed wetland ecosystems, which remain saturated throughout the year. Exploitation of ground water resources at a rate exceeding the rate of natural recharge would result in a lowering of the water table and, consequently, many groundwater seeps would dry up.

There is thus a need to develop environmental monitoring tools to better understand where decreases in wetland ecosystem performance are occurring and to assess the trends and possible impacts of groundwater extraction. Early detection of vegetation stress may be critical for the monitoring of plant ecosystems and how aquifer exploitation would influence them. Because of their multispectral character, broad scope and timeliness, satellite data have been very effective in monitoring the status of plant communities and the detection of the effects of stress and disease.

A Water Research Commission (WRC) research project entitled: "Ecological and environmental impacts of large-volume ground water abstraction in the Table Mountain Group (TMG) Aquifer systems" is being undertaken by a consortium of scientists from the Western Cape, led by Umvoto Africa, the CSIR and Southern Waters. The TMG-Eco project aims to identify and characterise TMG groundwater-dependent ecosystems and their sensitivity to variable boundary conditions, which include primarily large-scale water abstraction, but also climate change and loss of biodiversity. Evaluation of the potential impacts of water abstraction from TMG aquifer systems requires an understanding of the nature and extent of dependency of the ecosystems on this natural resource. One of the critical areas that will be addressed is the development of predictive tools and indicators to assess the impact of ground water extraction on the environment (Brown, Colvin, Hartnady, Hay, Le Maitre & Riemann 2003).

According to Brown *et al.* (2003), the methods to assess ground water's contribution to the ecosystem include the identification of groundwater discharge regimes and related water availability to terrestrial ecosystems. This can be achieved by either direct measurements in the field, or with the use of remote sensing techniques, or preferably, both.

1.2 STATEMENT OF THE PROBLEM

Due to the inaccessibility of many of the groundwater seeps and, consequently, the cost of direct monitoring by means of field observations, as well as the extended time scales involved, a means of remote monitoring of seep communities would be ideal for long-term ecosystem status assessment.

One of the ways of evaluating the degree of groundwater dependency of ecosystems is to assess the relative groundwater contribution to the ecosystem as a whole (Brown *et al.* 2003). This contribution can be assessed by means of remote sensing techniques, which would provide a means of monitoring the seasonal changes in wetlands, as well as the degree of moisture stress experienced by the different species during an annual cycle.

1.3 THE RESEARCH QUESTIONS

The objectives of the study can be summarised by the following research questions:

- Can groundwater dependent wetland communities be identified by means of satellite remote sensing techniques?
- Can the seasonal changes experienced by these communities be quantified using these techniques?
- Can the degree of groundwater dependency (i.e. ephemeral-, seasonal- or perennial dependency) be estimated?

The objective of the study is ultimately to establish the use of satellite remote sensing techniques to identify groundwater-dependent ecosystems and consequently those communities most likely to be affected by groundwater extraction. The ability to estimate the seasonal changes in these communities would imply that the proposed techniques could later be used for the development of monitoring tools for assessing the impact of groundwater extraction on the environment.

1.4 DESCRIPTION OF THE STUDY AREA

In order to understand the location of, and the changes experienced by, the groundwater-dependent wetland communities, it is necessary to consider the physical characteristics that will govern wetland formation within the study area. The physical characteristics that will influence the location of possible groundwater-dependent ecosystems are the geohydrological conditions in the area.

The Kogelberg Biosphere Reserve was selected for investigation because it was identified as one of the areas to be considered for assessing the possible impacts of large-scale groundwater abstraction on groundwater-dependent vegetation (Hartnady, Jackson & Riemann 2004). The reserve is situated approximately 30km to the east of Cape Point in the Western Cape Province, South Africa. The area investigated is included in the 3418 BD Hangklip 1:50 000 scale topographical map sheet. The map of the study area is presented in Figure **1.1**.

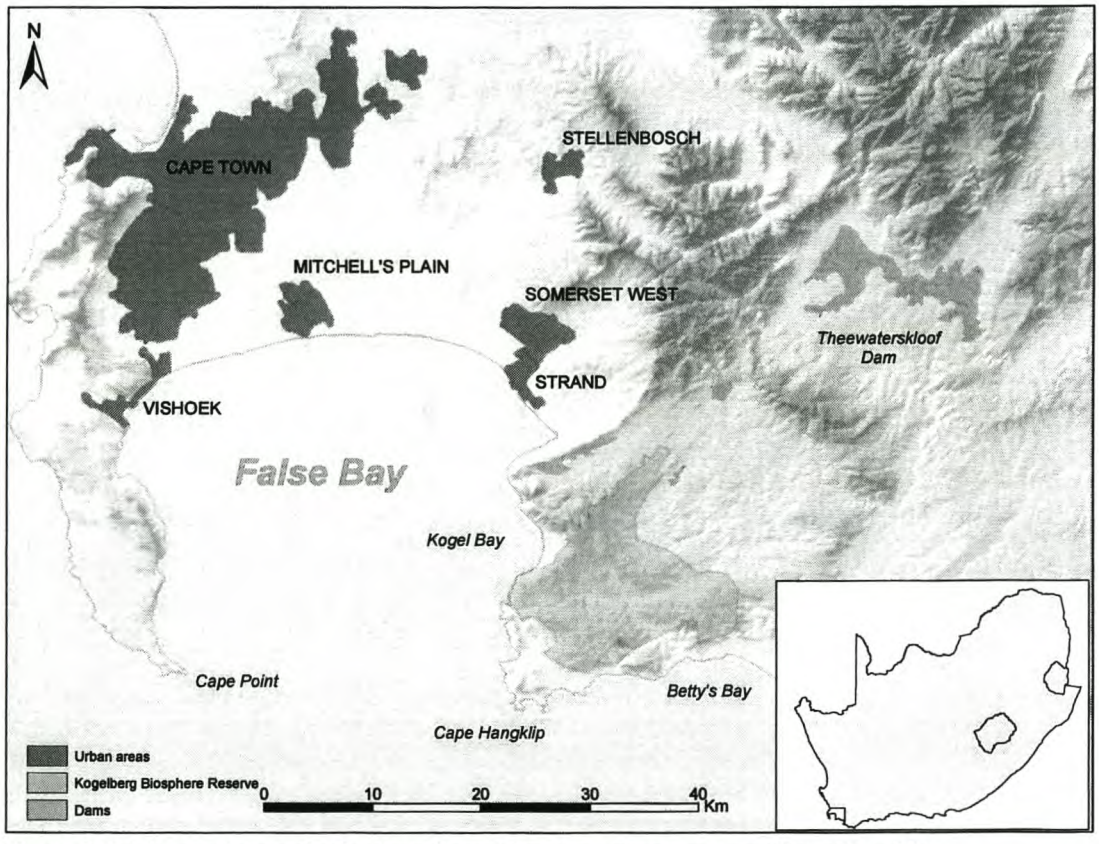

Figure 1.1: The study area in the Kogelberg Biosphere Reserve near Cape Hangklip.

The Kogelberg Biosphere Reserve extends from 0 to 1265m above sea level. Slopes range between 0 and 70 degrees, with the majority of the steep slopes (45 to 70 degrees) facing south to south-west. The reserve receives a total annual rainfall in excess of 1000mm, with the majority of precipitation occurring during autumn and spring (May to September). The annual temperatures range between a minimum of 12°C and a maximum of 23°C.

According to Boucher (1982), the sandstone mountains in the area support mainly typical Mountain Fynbos vegetation types (the vegetation map of the area is presented in Figure 1.2). The majority of the species in the area experience their growing season in the spring and summer, with productivity increasing sharply during this time. At the onset of winter (the wet season), the shorter days and colder temperatures will result in decreasing vegetation productivity. However, according to Weier & Herring (2001), vegetation growth and productivity are limited by water availability and, consequently, relative vegetation density would be a good indication of water availability. This means that during the relatively dry growing season, water availability to perennial wetland communities will result in these communities being discernable from the surrounding vegetated areas. This is due to the fact that the perennial wetland communities will be wetter and greener than the surrounding vegetation.

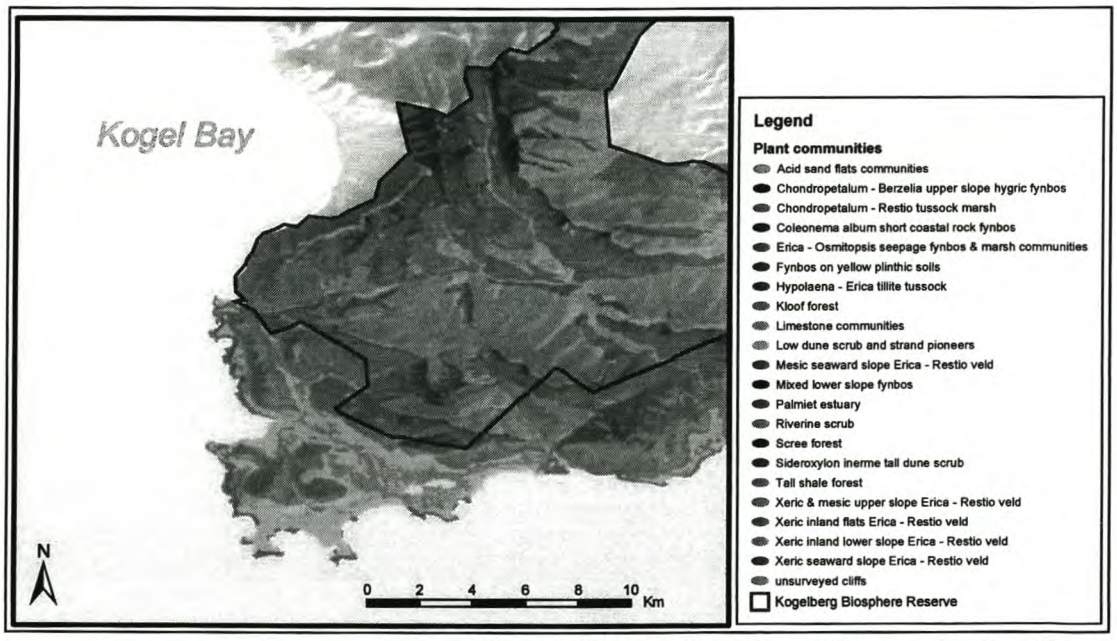

(Source: Western Cape Nature Conservation Board)

Figure 1.2: Vegetation of the Kogelberg Biosphere Reserve

The locations of groundwater-dependent ecosystems are governed by groundwater discharge from the water-bearing lithologies in the area. The geology of the study area is dominated by sediments of the Cape Supergroup, including the Table Mountain Group (TMG) and the Bokkeveld Group. The geology of the study area is shown in Figure 1.3.

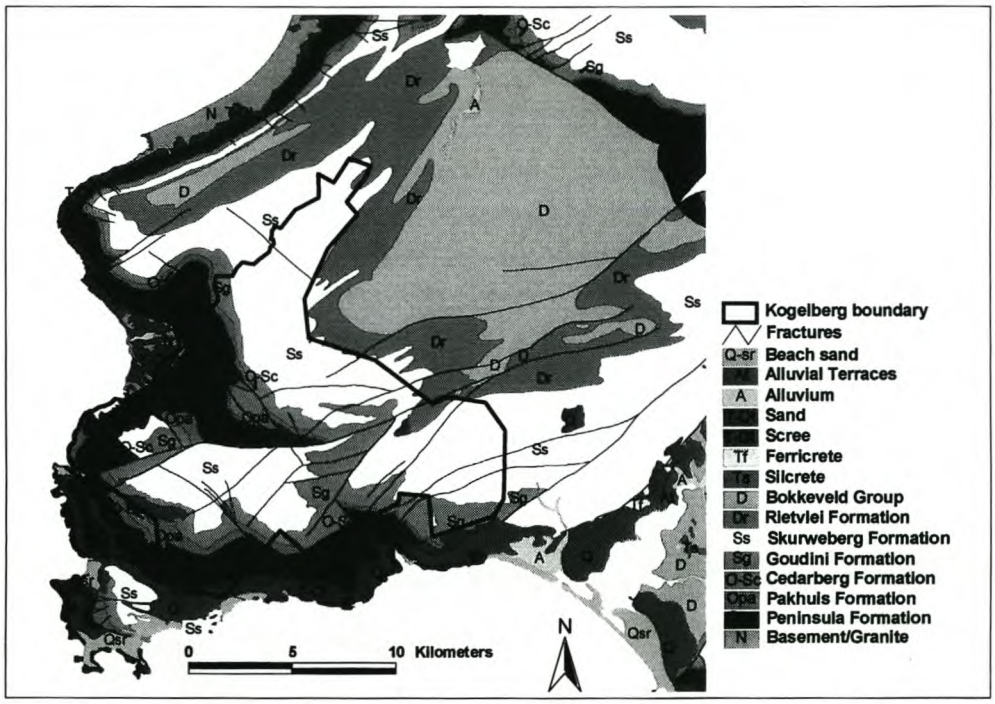

Source: ENPAT 2001

Figure 1.3: Geology of the Kogelberg area

The Peninsula and Pakhuis sandstone Formations are separated from the Goudini, Skurweberg and Rietvlei Formations (mostly consisting of quartzitic sandstones) by the Cedarberg Shale Formation. These formations form part of the TMG sediments and are overlain by the Gydo (predominantly shale) Formation of the Bokkeveld Group sediments (Theron, Gresse, Siegfried & Rogers 1992). The main groundwater-bearing lithologies considered for medium- to large-scale abstraction are the Skurweberg and Peninsula Formations (Brown *et al.* 2003).

The sandstones of the TMG are heavily fractured and folded, with the majority of these structures trending north-east or north-west. The major fault zones in the area are believed to provide preferred pathways for groundwater flow (Colvin, Le Maitre & Hughes 2002).

According to Colvin *et al.* (2002), groundwater discharge from the fractures results in complex discharge patterns with seepage areas occurring at various points along slopes, at changes in slopes as well as in localised flat areas. A typical TMG geohydrological setting is presented in Figure 1.4. Groundwater flow typically follows regional paths along fault zones and lithological contacts. Groundwater-dependent wetland ecosystems are likely to occur at the points where the groundwater discharges to the surface (Colvin *et al.* 2002).

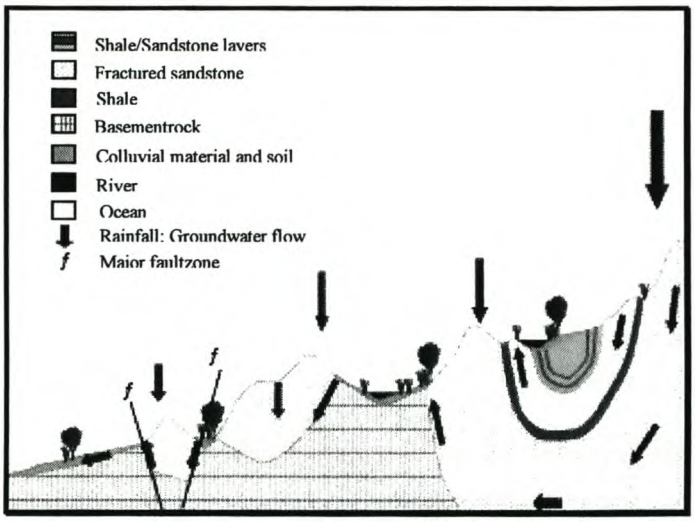

(Source: Colvin *et al.* 2002)

Figure 1.4: Fractured sedimentary terrain showing groundwater flow paths and groundwater dependent ecosystems

This type of geohydrological setting supports a range of groundwater discharge regimes, including ephemeral to wet-season only, and perennial springs and wetlands. This diversity of discharge regimes in turn supports a range of groundwater-dependent ecosystems with different sensitivities to changes in groundwater availability (Colvin *et al.* 2002). In this study references to non-perennial wetland communities should be taken to indicate any wetland communities that are not saturated throughout the year, including ephemeral and seasonal wetland communities. Perennial wetland communities refer to those communities that remain saturated throughout the annual cycle.

It is important to note that, according to Colvin *et al.* (2002), groundwater availability to a certain vegetation community does not necessarily imply groundwater dependence. Dependency on groundwater suggests that the ecosystem will be significantly altered if

groundwater availability was to change beyond its normal range of fluctuation. Although the study will concentrate on identifying wetlands with a likely component of groundwater interaction, these communities will be referred to as groundwater-dependent communities. The true nature of groundwater dependency, however, can only be assessed by water chemistry studies.

1.5 MATERIALS AND METHODS

1.5.1 Data requirements

The suitability of satellite imagery selected for use in a particular study can be assessed in terms of availability, spectral characteristics, spatial resolution and cost (Colvin *et al.* 2002). The Landsat 7 ETM+ imagery was chosen for this application because of its high spectral resolution (7 multispectral bands and one panchromatic band), while providing a suitable spatial resolution (30m resolution for the multispectral bands, and 15m resolution for the panchromatic band). Additionally, the 16-day revisit period provides multi-temporal image availability, while imagery can be acquired at reasonable cost from primary data suppliers.

The data requirements for the development and application of the proposed techniques are:

i. Satellite images of the region of interest (acquired from the Satellite Application Centre). These include images captured at the end of the dry period (where water stress is expected to be at a maximum) and at the end of the wet period (where water stress will be at a minimum);

ii. Vegetation and geological maps of the area of interest (acquired from the Western Cape Nature Conservation Board);

iii. A high-resolution digital elevation model (DEM), supplied by the Centre for Geographical Analysis, University of Stellenbosch.

1.5.2 Satellite image selection criteria

Groundwater-dependent wetlands in the area are expected to exhibit significant spectral differences to surrounding vegetation. This is due to the fact that perennial groundwater-fed wetlands are expected to remain water-saturated throughout the year, causing these wetland communities to remain wetter and greener, even after the dry season. Non-perennial wetlands and surrounding non-wetland vegetation communities are expected to experience a certain

degree of moisture deficiency, especially after the dry season. Therefore, multi-temporal images (at the onset of the wet season and at the onset of the dry season) for each year are desirable. For the selection of dates of image capture, a list of available weather stations and their monthly rainfall data was requested from the Institute for Soil, Climate and Water (ISCW) in Stellenbosch. The nearest weather station to the Kogelberg Biosphere Reserve (with data from 2000 to 2003) is the Oudebosch weather station. The location of this station as well as other weather stations in the area is presented in Figure 1.5.

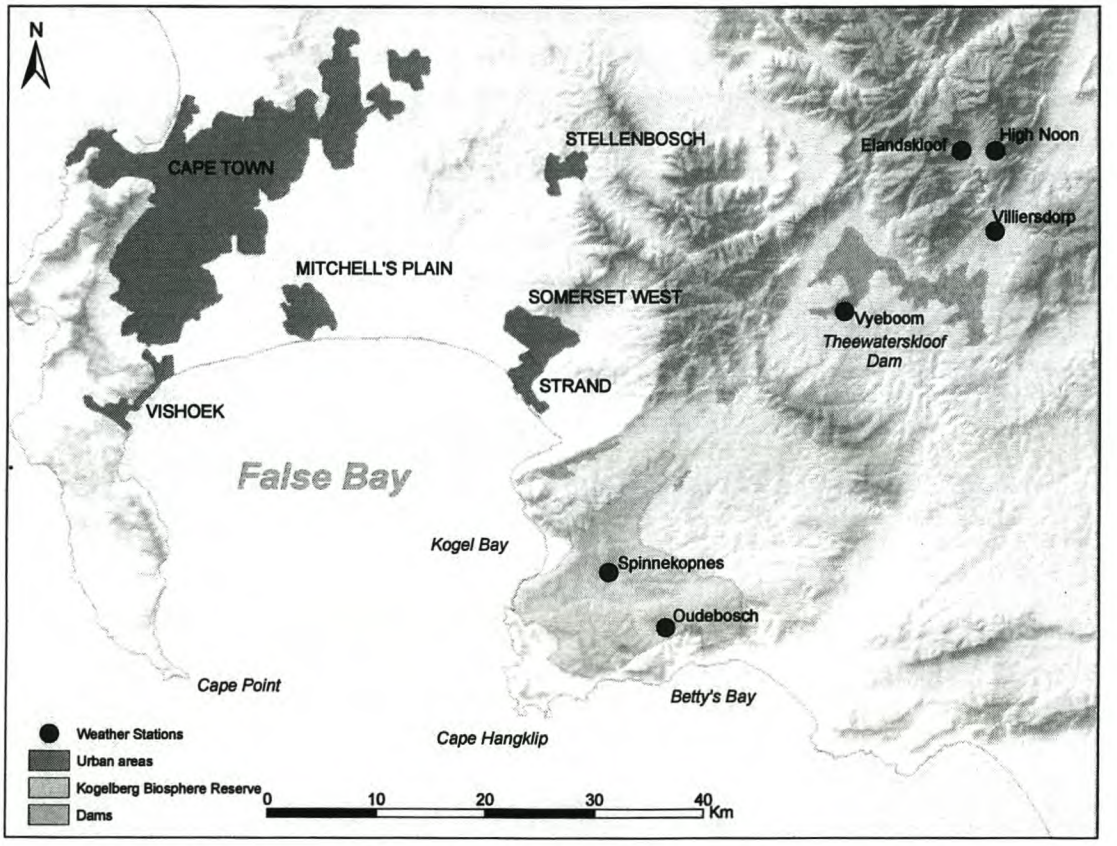

Figure 1.5: Weather station locations for the Kogelberg Biosphere Reserve and the surrounding areas

For the purpose of analysis successive end-of-wet period and end-of-dry period images should be selected. In order to estimate end-of-dry period and end-of-wet period conditions, the cumulative average rainfall for different sets of three successive months were computed to isolate the three-month period with the lowest average rainfall, as well as the period with the highest average rainfall. It is important (especially for the end-of-dry season data) to then obtain images captured on a date for which there was an extended period of low or no rainfall.

The daily rainfall data for the above chosen months were inspected in order to obtain these dates. The suitable dates for image capture are summarised in Table 1.1.

Table 1.1: Sets of dry and wet periods, and preferable capture dates for images

Year	Driest three months	End of dry period	Wettest three months	End of wet period
2000	Feb, Mar , Apr	9 – 19 May	Jul, Aug, Sep	2 – 8 Oct
2001	Jan, Feb, Mar	27 Mar – 1 Apr	Jul, Aug, Sep	27 Sep – 17 Oct
2002	Feb, Mar, Apr	1 – 3 May	Jun, Jul, Aug	30 Aug – 8 Sep
2003	Dec, Jan, Feb	1 – 6 Mar	Jul, Aug, Sep	7 – 11 Oct

After examining the Satellite Application Centre's online catalogue, three Landsat 7 images were chosen. The first was captured on 22 October 2001, which reflects the end-of-wet period conditions. The second image was captured on 18 May 2002 which represents the end-of-dry period conditions, while the third image, captured on 23 September 2002, approximates end-of-wet period conditions. Table 1.2 provides a brief description of imagery data obtained.

Table 1.2: Image data to be used for wetland change detection

Image Dates	**Landsat Sensor**	**Spatial resolution**	**Preprocessing level**	**Other**
21 Oct 2001 18 May 2002 23 Sep 2002	ETM +	30 m (Bands 1 - 6) 15 m Panchromatic 30 m Thermal	Level 1G: Geometrically rectified product free from distortions from sensor, satellite and earth	WRS: 175/84 UTM Zone 34, Ref. ellipse: WGS 84

1.5.3 Proposed image analysis strategies

1.5.3.1 Image preprocessing

The raw data collected by satellite sensors have both geometric and radiometric flaws. Radiometric corrections are necessary because remotely sensed data are affected by solar incidence angle, solar azimuth, earth-sun distance, viewing angle and atmospheric effects (Lück 2004; Munyati 2000). These factors combine to produce significant band-dependent radiometric differences that could influence the interpretation of both temporal and spatial

data sets (Huang, Yang, Homer, Wylie, Vogelman & DeFelice 2001; Irish 2000). When using Landsat imagery to map and monitor vegetation cover changes, it is desirable to remove these effects by methods which would produce a radiometrically consistent time-series of images. This enables indices or classifications derived for individual scenes to match other scenes both spatially and over time (Xiaoliang, Danaher, Wallace & Campbell 2001).

Geometric errors are caused by factors such as the earth's curvature and rotation as well as variations in the velocity, altitude and attitude of the sensor platform. Geometric correction is the step in correcting these errors in order to make data spatially consistent over time (Vergara s.d.). Systematic errors such as those introduced by the earth's curvature, as well as the yaw, pitch, roll, band alignment and sensor jitter from the satellite sensor are usually corrected by data suppliers selling level-1 processed imagery. Additional distortion introduced by topography and referencing of the image to an accurate geographic location has to be undertaken by the user (Lück 2004).

Additionally, the spatial resolution of Landsat 7 bands 1 - 5 and 7 is 30 meters. Considering the size of many of the wetlands in question, this resolution might prove to be too coarse for meaningful analyses. Image fusion, a method for combining the high spatial resolution of the 15 meter panchromatic band with the high spectral resolution of the multispectral bands (Zhang 2004), will prove to be a very important preprocessing procedure for wetland detection. Figure 1.6 is a diagrammatic illustration of the steps that will be taken during the image preprocessing stages.

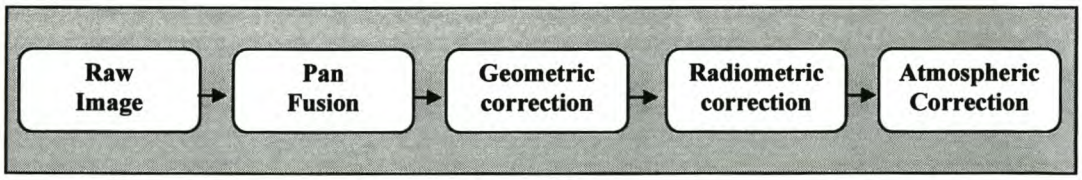

Figure 1.6: Steps involved in the image preprocessing

1.5.3.2 Image processing

After ensuring the radiometric and geometric comparability between data sets, various image analysis techniques will be employed in order to enhance latent information on vegetation productivity and moisture content of vegetation classes within the scene. Using the differential spectral properties of the vegetation classes of interest, the outputs of the different

image analysis strategies will be combined in a rule based classifier for discrimination between the vegetation communities of interest.

The image analysis strategies that will be employed to extract relevant vegetation-related variables will involve the following:

- *Band ratios/vegetation indices* derived from different combinations of spectral bands will provide a quantitative measure of various vegetation-related variables such as biomass and productivity, as well as soil and canopy moisture. When using productivity-related indices (such as the near infrared/red ratio) a high pixel value will reflect a condition with a high density of healthy vegetation, while lower values will indicate either a lower density of vegetation, or stressed vegetation. Moisture stress-related indices provided by the SWIR/NIR ratioing strategy will present a means of assessing the canopy and soil moisture within a pixel. Higher values will indicate lower moisture content, while lower values will be an indication of higher moisture content with a high possibility of wetland-related vegetation communities. Change vector analysis on the vegetation indices derived for different seasons within a year will present a means of assessing how the productivity and moisture content of the different communities fluctuates seasonally. Theoretically, since perennial groundwater-dependent communities remain saturated throughout the year, they would show a lesser degree of variation in productivity during an annual cycle, while also exhibiting a very low change in moisture stress index throughout the year.
- *Tasseled cap transformations* will be performed in order to derive the main components of vegetation, namely brightness, greenness and wetness. Especially the wetness and greenness components could prove to be useful for vegetation community discrimination. Greenness, like the vegetation productivity indices, will provide a measure of vegetation biomass, while the wetness component will present another means of assessing the moisture content within a pixel. Two images will then be compared, and change pairs computed by differencing images on each of the three tasseled cap components. The change vector then connects the same pixel as measured over two different times and the magnitude and direction of change can be interpreted (Lunetta, Johnson, Lyon & Crotwell 2004). For example, a pixel representing non-perennial wetland conditions would have a significant decrease in wetness when moving from end-of-wet period to end-of-dry period conditions, while perennial wetland communities would be expected to have a high wetness component throughout the year.

- *A rule based expert classifier* will be constructed using ERDAS Imagine's Knowledge Engineer. This classifier will enable the classification of perennial and non-perennial wetland communities. The classification of these general wetland communities will rely heavily on the output data layers produced during vegetation index derivation and tasselled cap transformation, and the various change detection results between the successive images. Based on the output of these general wetland communities, an attempt will be made to discriminate between different types of perennial wetlands, including those related to geological faults, and those occurring on lithological boundaries. Here additional ancillary data such as lithological boundary and fault data sets will be employed.

Campbell (1996) states that the high spectral, spatial and temporal resolution of satellite imagery data provides a means of monitoring vegetation health and productivity of vegetation classes over time. To determine the utility of Landsat 7 ETM+ data for the classification of vegetation/groundwater interaction, methods of data analysis, synthesis and comparison using remote sensing methodologies will be employed. The following chapter provides an introduction and theoretical background for the image analysis strategies employed for this study.

CHAPTER 2: LITERATURE REVIEW AND THEORY

2.1 INTRODUCTION

Long-term monitoring of ecological regions is a labour-intensive and time-consuming process, frequently requiring inaccessible areas to be covered by foot. Since vegetation vigour and productivity are continuously changing, monitoring would require frequent re-visitations, making this process virtually impossible to implement in practical terms. The use of remote sensing for the mapping and long-term monitoring of vegetation surfaces could overcome many of these limitations. It provides the analyst with the tools for monitoring the changes that takes place in ecosystems, with fieldwork being required only for the verification of results.

This chapter discusses the theory behind the various remote sensing and image analysis techniques for the detection and classification of groundwater dependent ecosystems used in this study. The use of vegetation indices and tasselled cap components in vegetation studies are reviewed, as well as how change vector analysis on these transformations can assist the classification process.

2.2 INTERACTION OF VEGETATION WITH ELECTROMAGNETIC RADIATION

Parker & Wolff (1965) noted that everything in nature has its own unique distribution of reflected, emitted and absorbed radiation. These spectral characteristics can be used to distinguish between different objects, or to obtain information about their shape, size and other physical or chemical properties. The variations in the amount of emitted and reflected energy across the electromagnetic spectrum are used to establish the spectral signatures for the given objects. The theory behind spectral signatures is that similar objects or classes of objects will have similar interactive properties with the electromagnetic radiation at any given wavelength, while different objects will have different interactive properties (Short 2003). A plot of the emitted or reflected result of these interactions against the different wavelengths would result in a unique curve, or spectral signature, that is diagnostic of the particular object (LP DAAC staff 2004).

Where vegetation is concerned, the use of the unique spectral curves associated with vegetated areas can be particularly effective for the assessment of various vegetation-related parameters. This is due to the fact that the pigment in plant leaves, chlorophyll, strongly absorbs blue and red visible radiation for use in photosynthesis, while strongly reflecting green radiation, resulting in the green appearance of plants (Campbell 1996; Short 2003; Weier & Herring 2001). Furthermore, the internal leaf structure of plants strongly reflects near infrared (NIR) radiation. These reflective/absorptive properties of vegetation provide a means of distinguishing vegetation from most other materials on a satellite scene. Healthy green vegetation would absorb most of the visible red light that it interacts with, while reflecting a large portion of NIR radiation, whereas unhealthy vegetation would reflect more of the visible light and less of the NIR radiation (Weier & Herring 2001). Additionally, the difference in reflectance between different plant species is most pronounced in the NIR portion of the electromagnetic spectrum, making discrimination between different vegetation classes a possibility (Campbell 1996).

Short (2003) states that spectral variability between species can also be a result of variable physical properties, including vegetation water content. Here, the short wave infrared (SWIR) radiation plays an especially important role. SWIR radiation is very sensitive to the presence of thin layers of soil and canopy moisture, with SWIR absorption increasing with increasing moisture content. This spectral property proved to be especially useful for the assessment and monitoring of wetland communities. Using a combination of SWIR and NIR reflective characteristics, moisture-deficient vegetation communities can be identified by their progressive decrease in NIR reflectance (decrease in productivity) as well as the increase in SWIR reflectance (decrease in moisture content) (Short 2003).

The interaction of electromagnetic radiation with vegetation has been used for various vegetation applications. Agricultural applications include the detection of stress as a result of moisture deficiency, pests and disease (Ceccato, Flasse, Tarantola, Jacquemoud & Grègoire 2001; Hatfield & Pinter 1993; Lelong, Pinet & Poilvè 1998; Moran, Clarke, Inoue & Vidal 1994; Zhang *et al.* 2003) as well as the determination of production estimates and crop yield (Doraiswamy, Hatfield, Jackson, Akhmedov, Prueger & Stern 2004; Shao, Fan, Liu, Xiao, Ross, Brisco, Brown & Staples 2001; Pradhan 2001; Tottrup & Rasmussen 2004). Other applications include the monitoring of desertification (Collado, Chuvieco & Camarasa 2002), fire-risk assessment (Mbow, Goïta & Bénié *et al.* 2004), and mapping forest stand age distribution (Zhang, Pavlic, Chen, Latifovic, Fraser & Cihlar 2004).

2.3 VEGETATION INDICES

The distinctive reflective properties of vegetation mentioned above allow for the classification of vegetation into different vegetation communities. Various physiological parameters, such as biomass and productivity, can also be quantified based on different combinations of satellite image bands (Viedma, Meliá, Segarra & Garcia-Haro 1997; Weier & Herring 2001). The various strategies that are employed to quantify the different vegetation-related parameters are collectively known as vegetation indices (Campbell 1996; Sims & Gamon 2003; Viedma *et al.* 1997). Various vegetation indices have been derived by using different combinations of spectral bands that are multiplied, divided, added or subtracted. The result of this image algebra would result in a single value that is indicative of the various plant physiological parameters within a pixel (Campbell 1996; Viedma *et al.* 1997; Weier & Herring 2001). According to Viedma *et al.* (1997), the close relationship between vegetation indices and the physiological plant parameters they estimate makes their use a valuable tool for monitoring and assessing vegetation conditions.

The most common image algebra strategy employed for the derivation of vegetation indices are band ratios. Band ratios are quotients between the reflectance values recorded in the different satellite image bands. Band ratios have been found to highlight certain absorptive and reflective properties of surface features, especially where there is an inverse relationship between the spectral responses for certain image bands (Campbell 1996). The inverse relationship between the reflectance of NIR and visible radiation for vegetation makes the ratioing strategy particularly effective for vegetation studies (Campbell 1996).

One of the many measures of vegetative vigour and abundance is the near infrared/red (NIR/R) ratio. Yet another measure employs the strong reflectance of green light by healthy green vegetation in a green/red band ratio. Some have found this index to be very effective, especially when the NIR band is unavailable (Gitelson, Kaufman & Merzlyak 1996), but others have found it less useful (Campbell 1996). The strong absorption of SWIR radiation by thin layers of canopy and soil water, and the high reflectance of NIR radiation by healthy green vegetation, provide another inverse relationship that can be effectively utilised, especially for the detection of wetland communities. The SWIR/NIR ratio, also referred to as the moisture stress index (Sims & Gamon 2003; Weier & Herring 2001), would then highlight areas with a high portion of healthy green vegetation, as well as a high moisture content, i.e. wetland vegetation communities.

Weier & Herring (2001) found that, using vegetation indices, satellite remote sensors can quantify what fraction of radiation used for photosynthesis is absorbed by vegetation. They state that scientists have found a direct relationship between the radiation that a plant absorbs and the net plant photosynthesis. The more a plant is absorbing visible light during the growing season, the more it is photosynthesising and, consequently, the more productive it is being. On the other hand, the less radiation a plant absorbs, the less the plant is photosynthesising and the less productive it is (Zhang, Qin, Liu & Ustin 2003). Either scenario results in a vegetation index value that, over time, can be averaged in order to establish the normal growing condition for the vegetation during the year. The measuring of plant productivity by means of vegetation indices can be used to characterise the health of vegetation during the year relative to the norm. In most climates vegetation growth is constrained by water availability, so that the relative vegetation density could be a good indicator of plant moisture stress (Hatfield & Pinter 1993; Weier & Herring 2001). According to Budde, Tappan, Rowland, Lewis & Tieszen (2004), vegetation degradation resulting from human pressures can be estimated by using vegetation indices, allowing assessment and monitoring of areas that are either consistently productive or degraded when compared to their surroundings.

According to Hatfield & Pinter (1993), the multispectral vegetation indices derived from vegetation reflectance values can be used to monitor the growth responses of vegetation in relation to measured or predicted climate variables. In this study seasonal variation in wetlands was used to assess the perennial or non-perennial nature of the wetland communities. Since perennial groundwater-fed wetland communities will remain saturated throughout the year, they will exhibit a lesser degree of variability in their productivity throughout the year. They will also have a lower degree of change in their moisture stress index when moving from end-of-dry period to end-of-wet period conditions, compared to surrounding vegetation.

Previous studies of vegetation indices applied for the monitoring and assessment of vegetation productivity include the use of vegetation indices for the quantification of photosynthetic tissues (Sims & Gamon 2002), the use of vegetation indices to assess vegetation re-growth after fire (Viedma *et al.* 1997), the use of the correlation between annual normalised difference vegetation index (NDVI) and rainfall as a signal of landcover performance (Urban 2000), as well as the use of NDVI together with local variance analysis for assessing vegetation degradation resulting from human pressures (Budde *et al.* 2004). The use of

thermal infrared (TIR) bands together with NDVI calculations has also demonstrated the ability to discriminate between senescent vegetation and bare soils (French, Schmugge & Kustas 2000).

2.4 THE TASSELLED CAP TRANSFORMATION

The tasselled cap transformation, also referred to as the Kauth-Thomas (KT) transformation, is based on a linear model similar to a principal component analysis (PCA), which considers the spectral variations common to a data set and separates the variability into discrete, non-correlated components (Levien, Fischer, Roffers & Maurizi 1998). The tasselled cap transformation reduces the ETM+ bands, excluding band 6, into six components, the first three of which correspond to the main components of vegetation. These are known as the brightness, greenness and wetness components, and are calculated from the reflectance values within a satellite scene (Huang *et al.* 2001; Urban 2000). The coefficients for the derivation of tasselled cap components for Landsat 7 imagery were developed by Huang *et al.* (2001) and are presented in Table 2.1.

Table 2.1: Coefficients for tasselled cap component derivation of Landsat 7 imagery

Index	Band1	Band2	Band3	Band4	Band5	Band7
Brightness	0.3561	0.3972	0.3904	0.6966	0.2286	0.1596
Greenness	-0.3344	-0.3544	-0.4556	0.6966	-0.0242	-0.2630
Wetness	0.2626	0.2141	0.0926	0.0656	-0.7629	-0.5388
Fourth	0.0805	-0.0498	0.1950	-0.1327	0.5752	-0.7775
Fifth	-0.7252	-0.0202	0.6683	0.0631	-0.1494	-0.0274
Sixth	0.4000	-0.8172	0.3832	0.0602	-0.1095	0.0985

(Source: Huang *et al.* 2001)

The brightness component is the weighted sum of all bands and is designed to capture the main trend of variation in soil reflectance (Levien *et al.* 1998; Urban 2000). This component is sensitive to changes in biological factors that would influence soil reflectance. Here the NIR band (Band 4) is weighted heavily, since this band is responsive to differences in soil brightness. The SWIR band (Band 5) is also weighted heavily due to its inverse response to soil moisture, which will affect soil brightness (Patterson & Yool 1998).

The greenness component is related to the amount of healthy green vegetation within a scene (Levien *et al.* 1998; Urban 2000). This component is a function of the NIR (Band 4)

reflectance from the internal structure of leaves, but also of the absorption and reflection of visible radiation by chlorophyll (Patterson & Yool 1998; Urban 2000).

Wetness, the third component, is associated with canopy and soil moisture (Levien *et al.* 1998; Urban 2000). The component contrasts the NIR band (Band 4) with the SWIR (Band 5) and mid infrared (Band 7) bands. This is based on the premise that increases in moisture will lead to a decrease in the amount of reflectance recorded by Bands 5 and 7, hence the negative signs in Table 2.1. The visible and NIR bands are less sensitive to variations in canopy and soil moisture, and contrasting these bands with Bands 5 and 7 accentuates moisture differences (Patterson & Yool 1998).

In this study, the tasselled cap components can be used in various ways for discriminating between wetland and non-wetland vegetation classes. Change vector analysis on the different tasselled cap components provide a means of summarising the change experienced within the pixel based on each of the tasselled cap components. The change vector inspects the same pixel on two different images, and the magnitude and direction of change between these two times can then be interpreted. Since perennial groundwater-fed wetland communities remain saturated throughout the year, they would exhibit only marginal variations in their wetness and greenness components during an annual cycle. Non-perennial wetland communities, on the other hand, would have a marked decrease in the wetness component when moving from end-of-wet period to end-of-dry period conditions. While all vegetation classes are expected to show an increase in greenness from the end of the wet period (end of winter) to the end of the dry period (end of summer - the growing season), the perennial wetland vegetation is expected to have a higher degree of productivity. This would be due mainly to the higher water availability for photosynthesis during the relatively dry growing season.

Tasseled cap transformations performed in conjunction with change detection strategies have been used extensively in many vegetation studies, including the monitoring of forest canopy changes due to drought (Collins & Woodcock 1996), stratifying land cover dynamics in terms of biomass loss and gain (Lorena, dos Santos, Shimabukuro, Brown & Kux 2002), monitoring vegetation cover change during two or more time periods (Rogan, Franklin & Roberts 2002) and the estimation of vegetation damage as a result of pests (Skakun, Wulder & Franklin 2003).

2.5 RULE BASED IMAGE CLASSIFICATION

According to Kidane (2004), classification of landcover classes based purely on the spectral characteristics of the features in question might be difficult, producing poor results. Some additional ancillary data might be useful for image classification and might significantly enhance the classification product. Knowledge-based expert classifiers provide a means by which the spectral characteristics of landcover classes may be used together with additional ancillary data for the purpose of landcover classification.

Ancillary data are defined as data generated by methods other than remote sensing analysis and can be used to assist in the classification of the landcover classes (Kidane 2004). The ancillary data that would prove useful for wetland classification include a geological map of the area of interest (including lithologies and faults), a digital elevation model (DEM) and the subsequent additional data layers that could be derived from these data sets. Additional image-derived data that were used for wetland classification in this study include the previously described tasseled cap component layers and vegetation productivity indicators, based on vegetation indices.

According to Kidane (2004), the knowledge/rule based classifier consists of three main elements:

- *The knowledge base* is a set of facts composed of imagery and ancillary data as well as a set of rules that describe the relationship between these facts;
- *The rules* are formalised during a training phase in order to identify distinguishable relationships between elements;
- *The recognition path* implies the problem-solving mechanism. It includes sets of production rules designed to access the knowledge base facts and rules. The recognition path controls the order in which rules are activated and used, and is most commonly implemented in the form of a decision tree.

The classification model is constructed by using two hierarchical levels. The first level, containing the basic models (BM), is the lowest level of the classifier structure. These models describe basic algorithms and rules which act as a recipe to create a data product. The explanatory variables that make up a basic model are analyzed statistically in order to identify suitable thresholds to identify the response variable. Relationships between the explanatory

and response variables can be described by expert knowledge of the features of interest. Where no expert knowledge exists, threshold values are determined by means of statistical analysis of training samples. The output results of the basic models can then be used within the second hierarchical level, the compound models (Kidane 2004).

Compound models (CM) are constructed by integrating several basic models and may take as input the output of other compound models. The compound models are designed to identify a single landcover class. The classification model is then defined by a sequence of compound models, keeping in mind that the order of execution of the models is important to ensure mutual exclusiveness of pixels. The basic hierarchical structure of the expert classifier is illustrated in Figure 2.1.

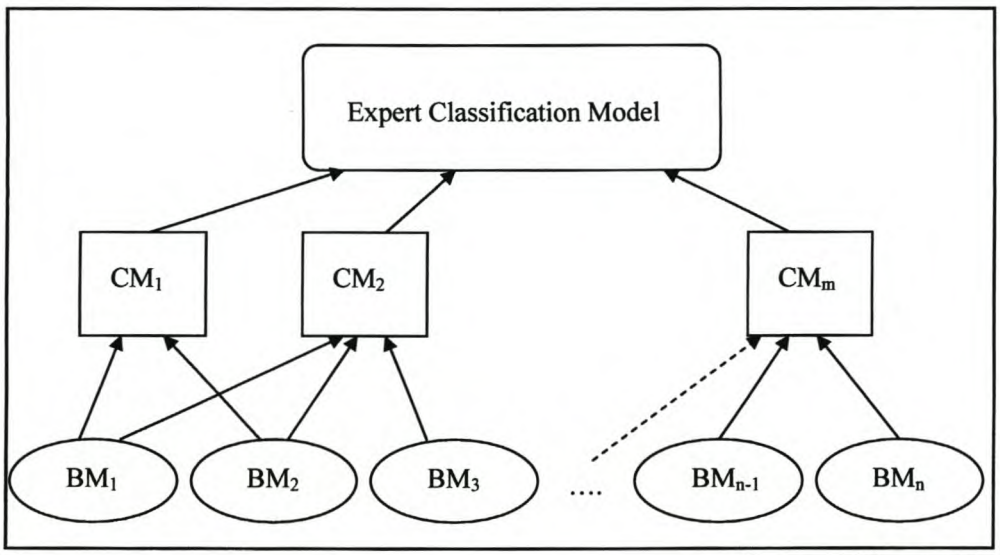

(Source: Kidane 2004)

Figure 2.1: Expert classifier structure (BM_n= Basic Model; CM_m = Compound model).

The expert classification models use various decision criteria and operations to identify the landcover classes of interest. Here certain pre-defined spatial operations (i.e. tasselled cap components and vegetation indices) are used for the construction of one or more basic models, which, in turn, are used to construct one or more compound models.

The past decade has seen significant research focussed on remote sensing techniques for various vegetation-related studies, with a number of different satellite- and aircraft-based sensors being used for this purpose. The use of Landsat 7 ETM+ data for the derivation of tasselled cap components and vegetation indices has been well documented and it is by means

of these transformations that a classification and assessment of groundwater interaction in vegetation communities were attempted. The ability to combine such image transformations with additional ancillary data for improving classification accuracy results will result in a method of identifying those vegetated areas with a high probability of groundwater interaction. The following chapter describes the image transformation procedures and the image classification process employed for this purpose.

CHAPTER 3: DATA ANALYSIS PROCEDURES

3.1 INTRODUCTION

The following chapter provides a description of the image processing procedures employed for this study, which can be summarised as follows (section numbers are indicated by brackets):

- Pan fusion; } 3.2.1.1 — 3.2.1
- Geometric correction and orthorectification; } 3.2.1.2 — 3.2.1
- Conversion of digital number (DN) images to radiance; } 3.2.1.3 — 3.2.1
- Conversion from radiance to reflectance; } 3.2.1.3 — 3.2.1
- Atmospheric correction; } 3.2.1.4 — 3.2.1
- Vegetation index derivation and change vector analysis; } 3.2.2.1 — 3.2.2
- Tasseled cap transformation and change vector analysis; } 3.2.2.2 — 3.2.2
- Rule based image classification. } 3.3

All analysis was performed using the Earth Resources Data Analysis System (ERDAS) image processing software, except for the pan sharpening and atmospheric correction procedures, which were performed using PCI Geomatica 9.1 software.

3.2 DATA PROCESSING

The ability to use remote sensing data to classify landcover classes is dependent upon the relationship between the remotely sensed reflectance values and the actual surface conditions (Munyati 2000). However, many external factors would influence the recorded pixel values. These include variations in sun illumination angle, earth-sun distance, atmospheric conditions as well as earth and sensor geometry (Lück 2004; Munyati 2000). Multi-temporal images are likely to be influenced differentially by these parameters and the images should therefore be normalised so that the effect of differing conditions could be eliminated, or at least minimised. Differences in values that arise from fluctuations in orbital and sensor characteristics are well documented and the necessary corrections are usually applied in the early stages of data collection by primary data suppliers (Lück 2004). For this study,

however, additional image preprocessing had to be performed by the user in order to ensure pixel-level comparability between images.

3.2.1 Satellite image preprocessing

The satellite data received from the data suppliers were subjected to Level 1 G preprocessing, meaning that the data were geometrically and radiometrically corrected. During Level 1 G processing the data undergoes two-dimensional resampling according to user-specified parameters such as output map projection. The Level 1 G product is considered to be free from distortions related to sensor movement (jitter, roll, view-angle effects), satellite movement (attitude deviations from nominal) and earth movement (e.g. rotation, curvature) (Irish 2000). These standard geometric and radiometric processing procedures result in digital number (DN) images, which represent the degree of at-satellite radiance.

The DN image data are usually affected by a substantial amount of noise, but a significant portion of the noise between images can be normalised by image preprocessing techniques (Huang *et al.* 2001). In order to compare images taken at different dates, images have to be matched radiometrically in order to account for variations in overall brightness and matched geometrically to ensure that pixels overlay precisely when images are compared. In addition, the pixel data will not only be influenced by sensor differences, but also by the accuracy of spatial registration of images, differences in atmospheric composition at the time of image capture and the spatial size of changes relative to the image resolution (Munyati 2000).

3.2.1.1 Image fusion for enhancement of spatial resolution

According to Zhang (2004), image fusion/pan sharpening is a method for the integration of the geometric detail of a high-resolution (15 meter) panchromatic image, with the radiometric detail of lower-resolution (30 meter) multispectral bands. This is done in order to derive a high spatial resolution image with a high spectral resolution. Since the spatial extents of the wetlands in question are expected to be less than 30 meters, this was compulsory for wetland detection.

The statistics-based image fusion module called PANSHARP, implemented in the PCI Geomatica 9.1 software package, was used for the fusion of the Landsat 7 multispectral bands

with the Landsat 7 panchromatic band. This module uses the least squares technique to find the best fit between the digital values of the image bands being fused and to adjust the contribution of individual bands to the fusion result to reduce the colour distortion. It also employs a set of statistical approaches to estimate the grey value relationship between all the input bands. This reduces the influence of dataset variation and automates the fusion process (Zhang 2004).

According to Zhang (2004), the PANSHARP module is expected to have a minimal colour distortion, as is evident in the Figure 3.1, which is the result of the image fusion process.

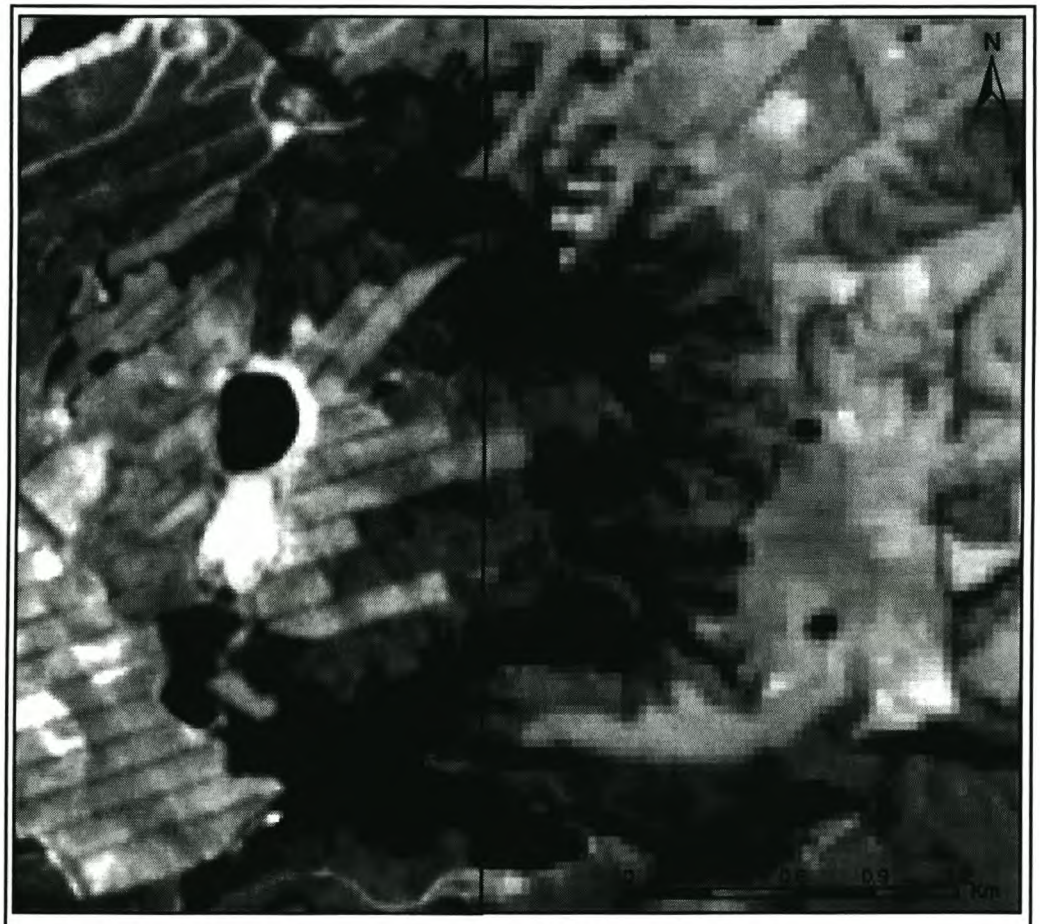

A: Pan-sharpened image B: Un-sharpened image

Figure 3.1: Comparison between a sharpened and un-sharpened multispectral image. Capture date: 22 September 2002. RGB = 453

3.2.1.2 Geometric correction

Levien *et al.* (1998) state that, when using satellite images for change detection, imagery must be co-registered to ensure that multi-temporal images from the same row and path are registered to within one pixel. This is achieved by on-screen identification of common features, such as road intersections. If pixels do not correspond completely, changes due to misregistration of pixels will be recorded in the final change map. According to Munyati (2000), geometric registration of a multi-temporal image set with RMS error of 0.25-0.5 pixel, or 1 pixel at most, is necessary for accurate change detection applications.

As mentioned earlier, the Level 1 G data were geometrically corrected. The geometric corrections employed by primary data providers ensure that the data are free from distortions caused by the Earth's rotation and curvature. However, according to Irish (2000), the 1 G correction does not employ ground control or relief models to ensure absolute geodetic accuracy. Consequently, as stated by Lück (2004), the removal of distortion introduced by topography and subsequent referencing of pixels to their accurate geographic location has to be undertaken by the user.

The ERDAS IMAGINE 8.7 Image Geometric Correction module was used for the geometric correction of the image. The Landsat geometric model was chosen, which allows for the orthorectification of Landsat data. A digital elevation model of the Western Cape (supplied by the Centre for Geographical Analysis, University of Stellenbosch) was used as elevation file. Fifty ground control points (GCPs) were collected on the *18 May 2002* image relative to a projected roads vector layer (1:50 000). A maximum root mean square (RMS) error of 9.0225 was achieved (refer to Table 3.1), ensuring that the data were accurate to within one pixel for the 15 meter resolution image, and less than a half a pixel for the 30 meter resolution images. The corrected *18 May 2002* image then served as reference image relative to which the *21 October 2001* and *23 September 2002* images were also corrected. The result of the image geometric correction and orthorectification is shown in Figure 3.2.

Table 3.1: Magnitude of error in orthorectification of images

Image	Pixel size after rectification	Total root-mean square error
22-10-01 (Panfuse)	15m	4.1477 (0.277 pixels)
22-10-01 (Original)	30m	5.5305 (0.184 pixels)
18-05-02 (Panfuse)	15m	9.0225 (0.602 pixels)
18-05-02 (Original)	30m	9.023 (0.301 pixels)
23-09-02 (Panfuse)	15m	2.1621 (0.144 pixels)
23-09-02 (Original)	30m	2.1822 (0.072 pixels)

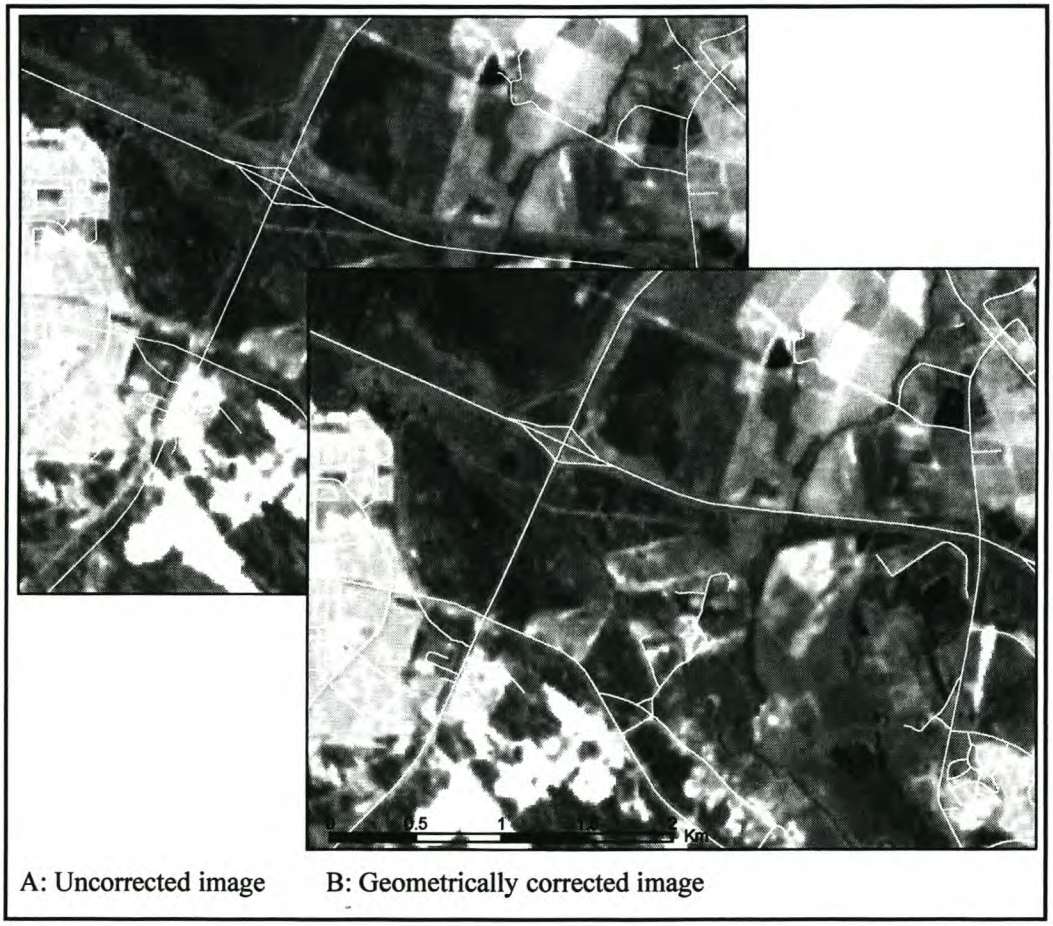

A: Uncorrected image B: Geometrically corrected image

Figure 3.2: Comparison between the geometrically corrected and uncorrected images. Capture date: 22 September 2001. RGB = 432

According to Irish (2000), the residual error in the systematic Level 1 G product is approximately 250 meters in flat areas at sea level. The correction and orthorectification of the images using GCPs reduced the geodetic error of the output images to less than 15 meters, ensuring pixel-level comparability between images.

3.2.1.3 Radiometric calibration

In order to standardise the impact of illumination geometry on the 8-bit digital number (DN) imagery, it first had to be converted to at-satellite radiance, and then to at-satellite reflectance, using information extracted from the imagery header files.

The formula for the conversion of digital numbers to at-satellite radiance can be expressed as:

$$L_\lambda = (gain_\lambda \times DN_\lambda) + bias_\lambda$$ (Source: Irish 2000),

where L_λ is the at-satellite radiance for band λ, gain and bias are the band-specific gain and bias values extracted from the image header files, and *DN* is the band-specific digital number values of the uncorrected image.

Conversion from at-satellite radiance to at-satellite reflectance will ensure inter-scene standardization for effects, including Earth-Sun distance and solar elevation angle. The conversion can be expressed as:

$$\rho_\lambda = \frac{\pi \times L_\lambda \times d^2}{ESUN_\lambda \times \sin\theta}$$ (Source: Irish 2000),

where ρ_λ is the unitless at-satellite reflectance, L_λ is the at-satellite radiance, d is the Earth-Sun distance (extracted from imagery header files), $ESUN_\lambda$ is the band-specific mean solar exoatmospheric irradiance (Table 3.2), and θ is the solar elevation angle (extracted from imagery header files).

Table 3.2: ETM + Solar spectral irradiances

Band no.	1	2	3	4	5	7	8
Irradiance	1969.000	1840.000	1551.000	1044.000	125.700	82.0700	1368.000

(Source: USGS 2001)

Landsat 7 thermal infrared bands (Band 6) can also be converted to at-satellite temperatures of the viewed Earth-atmosphere system under the assumption of uniform emissivity and using the pre-launch calibration constants listed in Table 3.3. The formula for this conversion can be expressed as follows:

$$T = \frac{K2}{\ln\left(\frac{K1}{L_\lambda} + 1\right)}$$ (Source: Irish 2000)

Where T is the Effective at-satellite temperature in Kelvin, *K1* and *K2* is calibration constants 1 and 2 from Table 3.3 and L is the spectral at-satellite radiance.

Table 3.3: ETM+ thermal band calibration constants

Constant 1 (K1) in watts/(m^2 * ster * μm)	Constant 2 (K2) in Kelvin
666.09	1282.71

(Source: Irish 2000)

3.2.1.4 Atmospheric correction

Electromagnetic radiation (EMR) undergoes significant interactions with the atmosphere before it reaches the earth's surface, and again as it moves from the earth's surface to the satellite sensor. Essentially, two processes affect the propagation of EMR through the atmosphere, namely absorption (where radiation is absorbed by particles in the atmosphere, and later re-emitted at different wavelengths) and scattering (where EMR is redirected due to particles in the atmosphere). The type and significance of the scattering depends upon the size of the scattering element compared to the wavelength of the radiation. This could have significant effects on an image, especially in the visible bands. These effects are observable as haze within a satellite image scene (Pani 2001). According to Chavez (1988), the influence of scattering on the visible and near-infrared bands is an additive effect on the radiation reaching the satellite sensor, thereby increasing the recorded reflected radiation. It must therefore be compensated for when investigating reflective properties of ground features over time. Consequently, any image processing techniques that analyze the spectral response of different spectral bands will be affected by the composition of the atmosphere at the time of image capture (Pani 2001).

The spectral response of the vegetation classes of interest (wetland vs. non-wetland vegetation) will be affected by the changing atmospheric conditions at the different times of image capture. Since seasonal data will be analysed, different atmospheric conditions are expected to influence the different images. To ensure that observed seasonal changes are a result of actual changes on the ground and not due to variable atmospheric conditions, the image data used need to be atmospherically corrected and normalised.

Several techniques have been developed to compensate for atmospheric scattering and effective haze removal. According to Coppin (2002), these techniques are grouped into three broad categories.

- First-order corrections rely on recorded reflectance values of scene features of known or assumed brightness. Certain assumptions, not always applicable to the case at hand, are made. These assumptions include uniformity of haze degradation over the entire scene, the additive character and wavelength dependency of atmospheric scattering, as well as the equal effect on all pixel brightness values. Examples include the dark object subtraction technique, which involves the identification of the lowest pixel value within an image. The pixel is then assumed to have a reflectance value of zero and the recorded deviation from zero then represents the additive atmospheric component, which can be subtracted from the entire image (Chavez 1988; Coppin 2002; Song, Woodcock, Seto, Lenney & Macomber 2001).
- The second category also uses reflectance values of features with known or assumed brightness, but also attempts to exploit the knowledge of the relationships between the separate spectral bands. An example of such a technique is regression analysis, where a best-fit line of plots for pixels within homogeneous cover types is determined. The slope of the line would then be representative of the ratio of reflected radiation (Coppin 2002).
- The third category of procedures attempts to model the physical behaviour of EMR as it passes through the atmosphere. Here detailed meteorological information is required, but since data on atmospheric humidity and concentration of atmospheric particles are difficult to obtain in the necessary detail, these techniques are not routinely used. One example of such a model (ATCOR 2) was developed by Dr Richter of the German Aerospace Centre (DLR) (PCI Geomatica V9.1 online help). This model includes certain pre-defined atmospheric conditions (based on geographic

location and seasonal climate variables), which are stored in a database. For the implementation of this model, only ancillary data related to satellite gains and bias values, solar zenith angle and sun elevation (which can be extracted from the imagery header files) are needed for each image.

It is important to note that the ATCOR 2 algorithm, as implemented in the PCI Geomatica v9.1 software, takes radiometrically uncorrected digital number images as input. Radiometric normalisation by conversion of DN images to radiance, and then to at-satellite reflectance is implemented within the algorithm. This means that, if the user intends to employ the ATCOR 2 algorithm for atmospheric corrections, the radiometric preprocessing procedure, as described in Section 3.2.1.3, would not be necessary.

The ATCOR 2 atmospheric correction algorithm employed in PCI Geomatica v9.1 was applied to each image by using the atmospheric correction functions stored in the database look-up tables. The model assumes a flat terrain consisting of horizontal surfaces. Input parameters for the model include the specification of a calibration file (extracted from the image header files), as well as an atmospheric definition that can be chosen from a list of pre-defined atmospheric conditions. Haze and cloud were also removed from the images by means of the following statistical haze removal algorithm:

1. Firstly, the scene is partitioned into clear, haze and cloud regions. Haze and clear areas are masked by means of the fourth tasseled cap component, which can be calculated by $TC_4 = (x_1 * B_1) + (x_2 * B_3)$, where B_1 and B_3 are the blue and red bands respectively, while x_1 and x_2 are their respective weighting coefficients (Table 2.1). Clear (or haze-free) pixels are then defined as those pixels with a TC_4 value of less than the mean TC_4 value for the entire image. Cloud areas are masked in order to exclude them from the haze regions, since surface reflectance information cannot be retrieved from these regions. The haze and cloud masks derived during this process are presented in Figure 3.3.

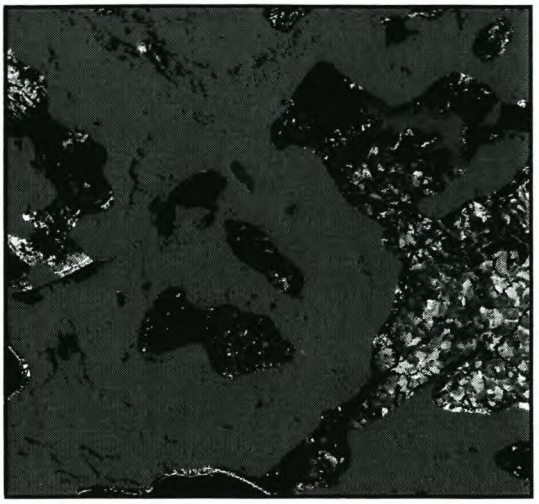

Figure 3.3 Haze mask (green) and cloud mask (red) generated by the ATCOR 2 module. Capture date: 22 September 2001.

2. Linear regression of the pixel values of B_3 and B_1 for the clear regions provides a line representing the clear sky vector. The direction of the clear sky vector can be expressed by its slope angle (θ). An increase in atmospheric contamination will manifest itself by increasing deviation from this clear sky vector. An example of a clear sky vector generated from the 22 September 2002 image is presented in Figure 3.4.

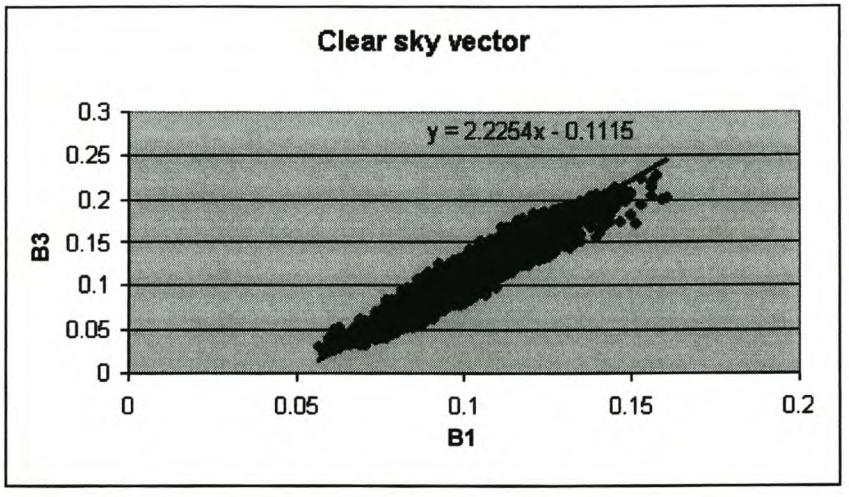

Figure 3.4: Clear sky vector for cloud free area.

3. The transformation that quantifies the perpendicular displacement of a pixel along the clear line can then be calculated by $HOT = B_1 \sin\theta - B_3 \sin\theta$ where B_1 and B_3 are the digital numbers of the blue and red bands respectively. This transformation is applied to each pixel in order to generate a HOT (Haze Optimized Transformation) image, which is a representation of the haze variation within a scene.

4. For each spectral band, the histograms of the haze regions are matched to the histograms of the haze-free and cloud-free regions. Here the assumption is made that the statistical properties of the hazy part of the scene are the same after haze removal as the statistical properties of the non-hazy part.

5. The last step involves the conversion of digital numbers to reflectance values.

The output of the ATCOR 2 algorithm is a satellite image in which atmospheric effects are removed, thereby retrieving the actual physical parameters of the earth's surface, i.e. surface reflectance. The atmospherically corrected output in comparison with the atmospherically uncorrected image is shown in Figure 3.5 a and b respectively.

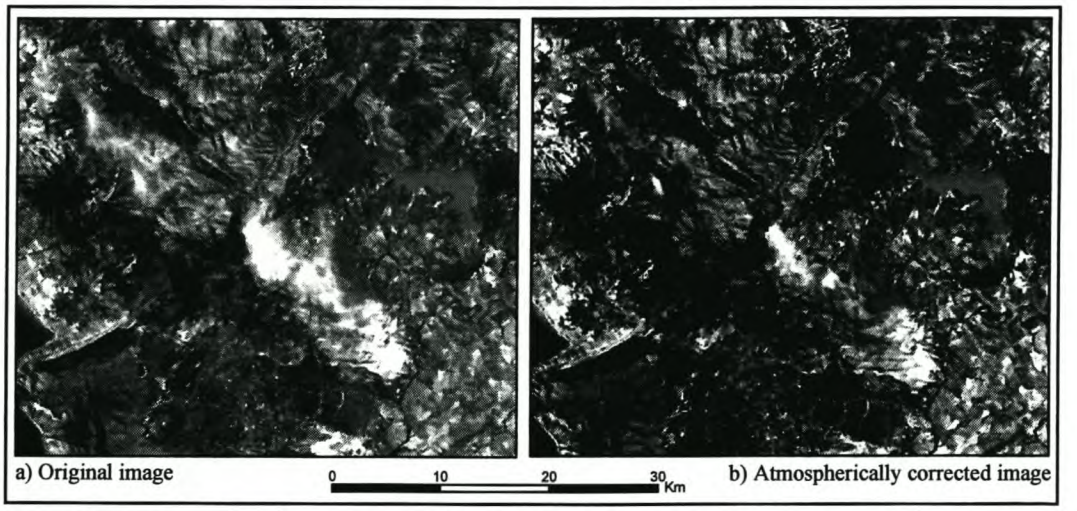

Figure 3.5: Comparison between the original (a) and atmospherically corrected (b) images. Capture date: 22 September 2002; RGB = 321

3.2.2 Image processing and analysis

3.2.2.1 Derivation of vegetation indices

The band ratioing strategy was used for the derivation of the vegetation indices. Of the two band ratios that were employed, the first was based on the NIR reflection and the visible red absorption of productive vegetation. This band ratioing strategy has been used extensively in vegetation studies, more commonly in the form of the normalised difference vegetation index (NDVI), which can be expressed as:

$$NDVI = \frac{NIR - R}{NIR + R}$$ (Source: Urban 2000)

The NIR/R ratio in this form partially normalises the effects of external factors associated with illumination variations such as the change in sun angle and atmospheric degradation (Urban 2000; Weier & Herring 2001). Since radiometric normalisation and atmospheric correction of the satellite imagery during the image preprocessing phase resulted in images free from these distortions, the NIR/R band ratio in its simple form was derived. The result of this band ratioing strategy resulted in a single-band image in which the value within a pixel is related to the amount of productive vegetation in that pixel. The output is presented in Figure 3.6.

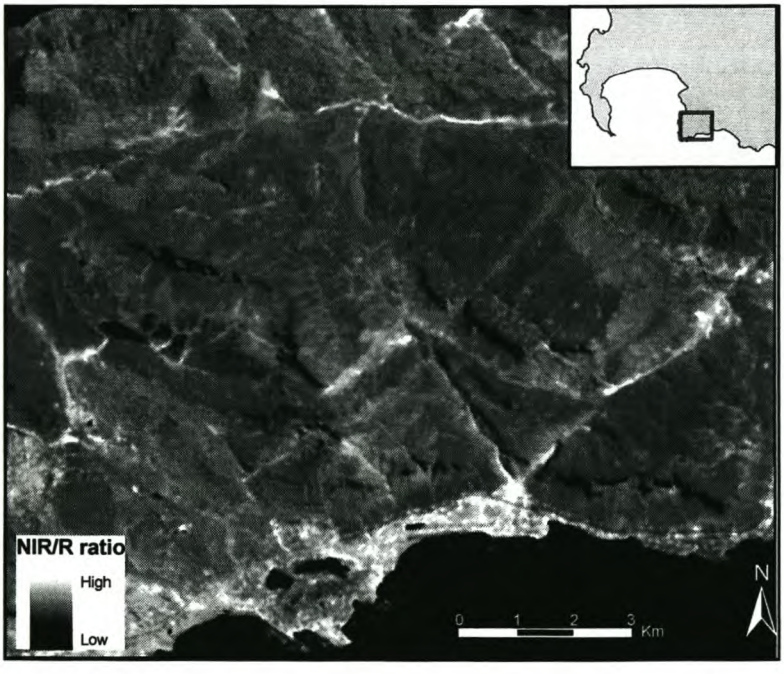

Figure 3.6: Grey-scale image representing the NIR/R (productivity) index. Capture date: 22 September 2001.

Change vector analysis on the vegetation indices for the different seasons provided an indication of the variance in productivity of the different communities within an annual cycle. When moving from end-of-wet period to end-of-dry period conditions, one would expect an overall increase in productivity of all vegetation communities, since the end of the wet period corresponds with the start of the growing season. However, according to Weier & Herring (2001), the amount of photosynthesis and consequently productivity is directly related to water availability. This implies that wetland communities, which still remain saturated during the dry summer period, would exhibit a higher degree of productivity in comparison with the surrounding non-saturated vegetation. When moving from end-of-dry period to end-of-wet period conditions, one would expect an overall decrease in productivity of all vegetation communities, since the end of the dry period corresponds with the start of the winter season. The colder, shorter days result in vegetation communities becoming senescent, and consequently less productive. The result of the change vector analysis for the end of the wet period to the end of the dry period is presented in Figure 3.7.

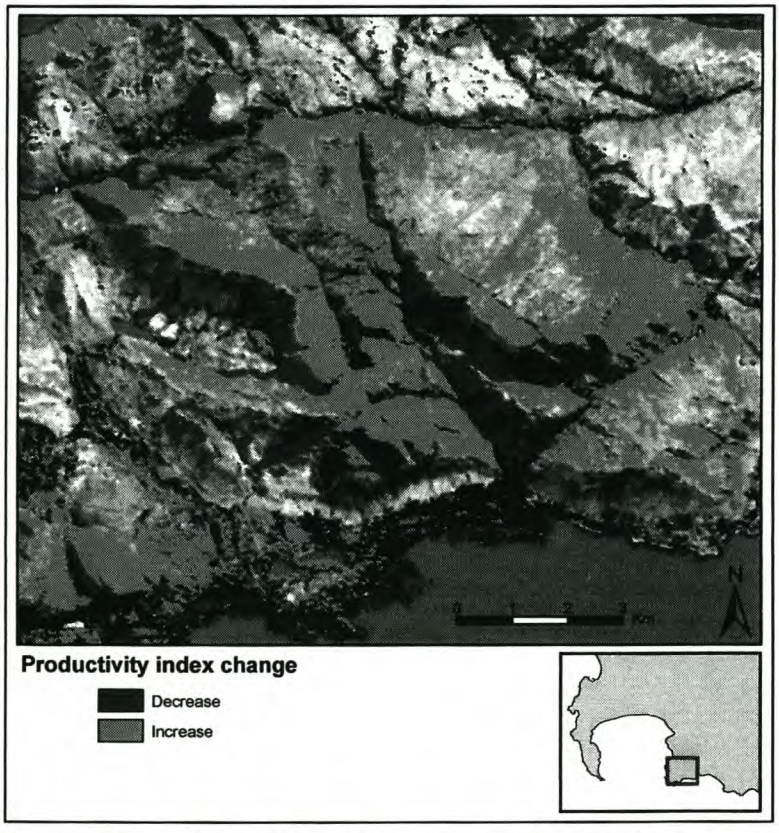

Figure 3.7: Highlighted NIR/R change image. 22 September 2001 to 18 May 2002.

The decreasing productivity exhibited on the south facing slopes is misleading. These areas are located in the shadows of the mountains on the 18 May 2002 image meaning that the spectral responses of the pixels could not be retrieved. These areas were masked out of the final wetland classification procedure.

The second band ratios that were derived are based on the inverse relationship between SWIR and NIR radiation of wetland communities. Since wetland communities will still have a high NIR reflectance, but a high SWIR absorption relative to non-wetland communities, this ratioing strategy would provide a means by which non-wetland vegetation could be distinguished from wetland vegetation. These ratios, also referred to as moisture stress indices, would provide a quantitative measure of the moisture content of the soils and canopies. A high ratio value would indicate a low amount of moisture for productive vegetation, while a low ratio value would indicate high moisture content for productive vegetation. The result of the SWIR/NIR ratio is presented in Figure 3.8.

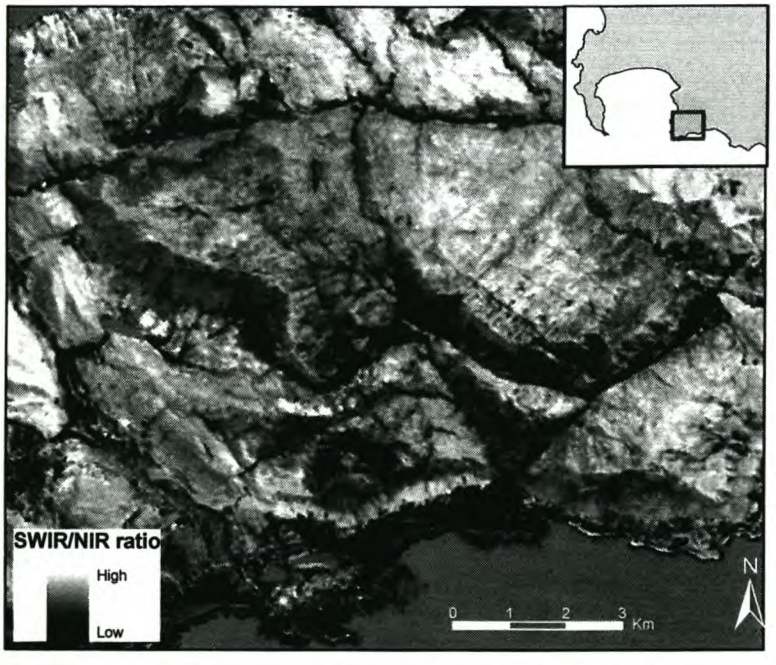

Figure 3.8: Grey-scale image representing the SWIR/NIR ratio (Moisture stress index). Capture date: 22 September 2001.

Change vector analysis on the moisture stress index images would provide a means of assessing the relative moisture content change within a pixel. Perennial wetland communities would be indicated by a relatively constant moisture stress index throughout the year, while

non-perennial wetlands would show a decrease in moisture stress index when moving from end-of-dry period to end-of-wet period conditions (meaning an increase in moisture content). The same non-perennial wetland communities would exhibit an increase in moisture stress index when moving from end-of-wet period to end-of-dry period conditions (decrease in moisture content). The result of the change vector analysis on the moisture stress index from the end of the wet period to the end of the dry period is presented in Figure 3.9.

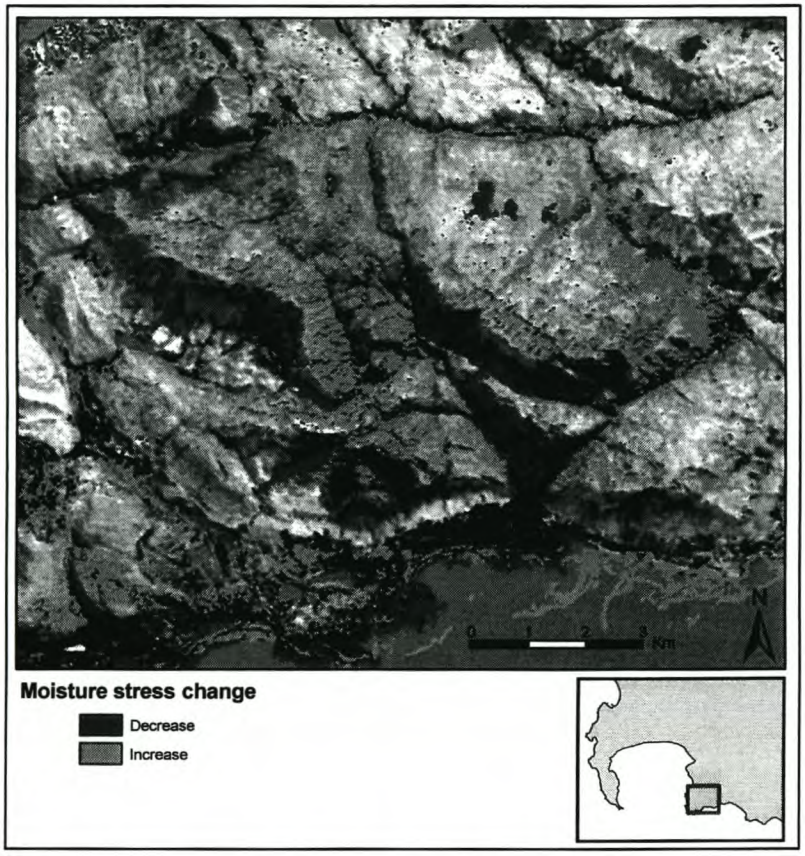

Figure 3.9: Highlighted moisture stress index change image. 22 September 2001 to 18 May 2002.

The decreasing moisture stress exhibited on the south facing slopes is misleading. These areas are located in the shadows of the mountains on the 18 May 2002 image meaning that the spectral responses of the pixels could not be retrieved. These areas were masked out of the final wetland classification procedure.

Where productivity is concerned, one would expect that an increase in water availability will go hand in hand with an increase in productivity. This is true for most vegetated surfaces, but because the Western Cape is associated with winter precipitation, this assumption cannot

always be made. Higher productivity associated with the wet season cannot be assumed in this case, since the wet season is also the winter season, implying that the vegetation communities will become senescent. However, the productivity index was compared to the moisture stress index and a high negative correlation was found between both the end-of-wet period to end-of-dry period change vectors (Pearson r = -0.96), and the end-of-dry period to end-of-wet period change vectors (Pearson r = -0.93). This means that a decrease in moisture stress index (increased moisture content) could be associated with an increase in productivity index (increased productivity).

3.2.2.2 Calculation of tasselled cap components

The tasselled cap transformation was computed using the Landsat 7 weighting coefficients (Table 2.1) for the reflectance values for each of the three images. Only the second (greenness) and third (wetness) components from the output transformations were used for further analysis. Change detection was performed between the greenness and wetness layers for each of the successive images. This created two successive greenness difference images as well as two successive wetness change images. The result of the change detection strategy for end-of-wet period to end-of-dry period conditions is presented in Figure 3.10.

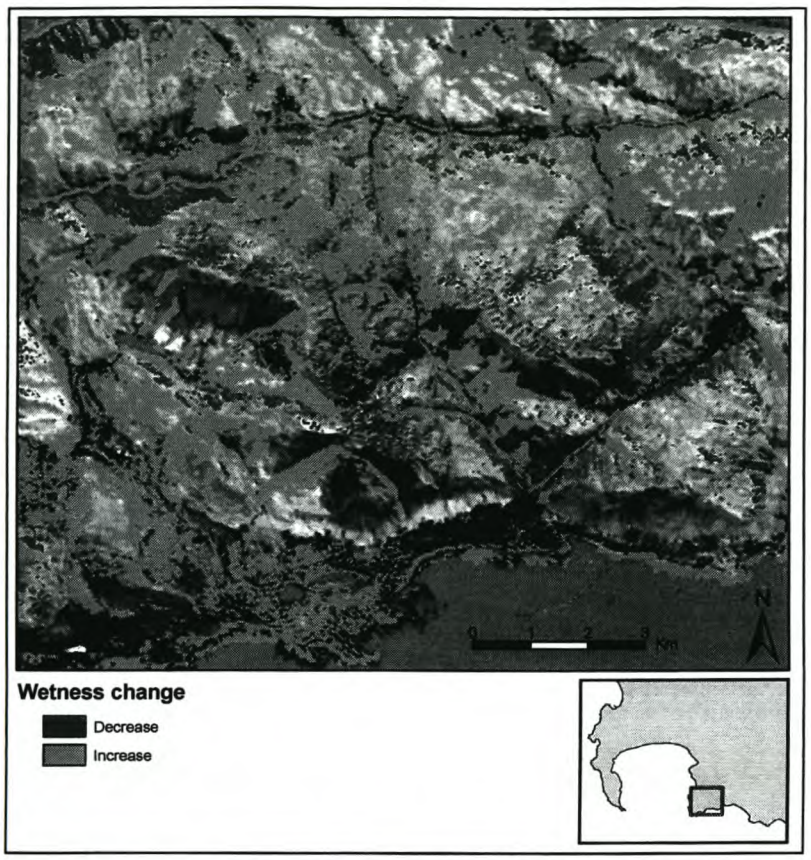

Figure 3.10: Highlighted change image for the wetness tasselled cap component. 22 September 2001 to 18 May 2002.

Positive changes in the greenness component in two successive images suggest an increase in productivity of vegetation over time, while a decrease in the greenness component will reflect a lesser degree of productivity, possibly a result of moisture deficiency (Viedma *et al.* 1997). Wetness component changes, on the other hand, will provide an indication of water availability during two successive seasons. A decrease in wetness component would be an indication of a decrease in water availability from one season to the next, while an increase in wetness would indicate increased water availability.

Like the productivity index, a greenness increase associated with increased wetness cannot be assumed, since the vegetation communities are associated with a winter precipitation climate. Here the wet season corresponds with the winter period, meaning that most vegetation communities will become senescent. When correlating change in wetness and change in greenness, only a weak correlation was found for both change results (end-of-wet period to

end-of-dry period Pearson r = -0.69; and end-of-dry period to end-of-wet period Pearson r = -0.19)

3.3 RULE BASED IMAGE CLASSIFICATION

The sample data used for training and thresholding purposes was obtained from a vector layer containing GPS coordinates of known wetland communities, collected by researchers during 2005. Overall, 23 known wetland communities were identified, 7 of which were randomly selected to serve as training datasets. The training sites were converted to 9 by 9 pixel areas of interest and used to extract the pixel data and spectral responses from each of the data layers. Of the remaining 16 sites, 9 could not be used due to the fact that these where located within the shadows of mountains on the dry period image, or underneath the masked out cloud regions on the 23 September 2002 image. Spectral data could not be extracted from these areas and, consequently, these areas could not be classified. The remaining 7 wetland communities were used at a later stage to test classification accuracies. Threshold values were estimated by investigating the statistics (minimum, maximum and mean values) of the pixel data for each of the 7 training sites. The wetland communities used for training and reference data, as well as those that could not be classified is presented in Figure 3.11.

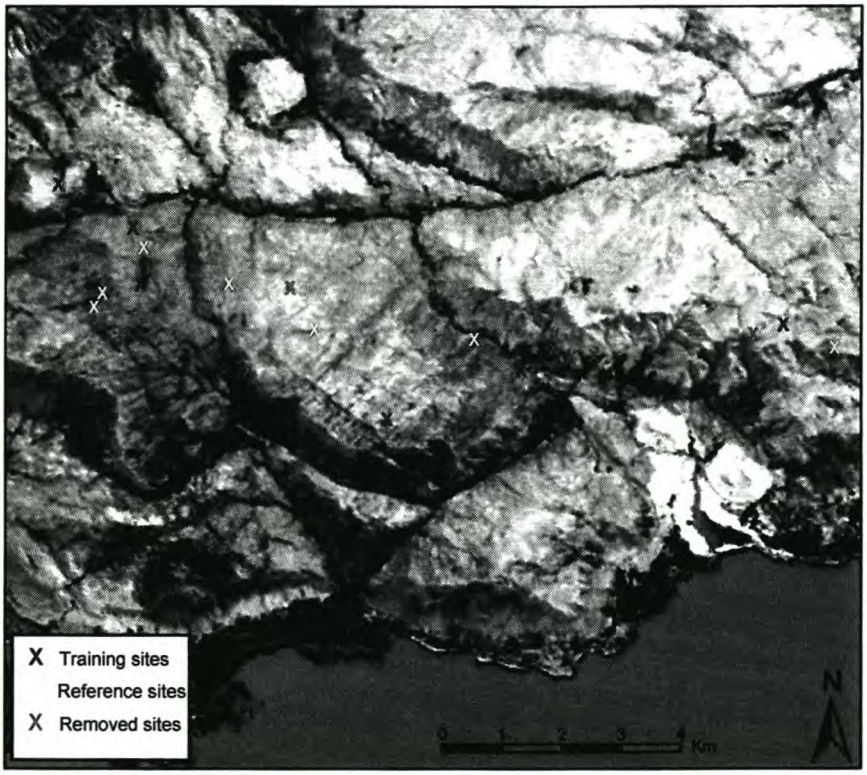

Figure 3.11: Field data used for training and accuracy assessment

An attempt was made to discriminate between six wetland categories, the first two of which represent general perennial and non-perennial wetland communities. After identifying perennial wetland communities, this category was refined to differentiate between two types of wetlands related to certain geological conditions. They include wetlands related to geological faults, and those that are related to contacts between different geological formations. These geological features are believed to be a source of groundwater discharge, and consequently these communities are likely to be dependent on water supplied by the TMG aquifer. Since lithological boundaries and faults frequently coincide, the third class was designed to identify those wetlands that are related to both faults and lithological boundaries, and hence those areas with a very high probability of groundwater interaction. However, not all perennial wetland communities can be expected to coincide with these geological conditions and, consequently the fourth category will include those pixels that were classified as perennial wetlands, but which do not coincide with the predefined geological conditions. The fifth class was designed to identify those wetland communities with only seasonal groundwater availability. This means that these communities will remain saturated for the duration of the wet period, but will dry up during the dry period. The final class was designed to identify the wetland communities that will form as a result of surface water accumulation, including rainwater accumulation. These wetlands are not expected to have a significant amount of groundwater interaction, but the degree of interaction can only be estimated by water chemistry investigations.

ERDAS Imagine 8.3's Knowledge Engineer was used for the construction of the rule based classifier. A classifier is constructed using three main elements: 1) variables, which represent the image data products derived during the image processing stage; 2) rules, which describe the conditions pertaining to the variables in order to place them within a certain class (also known as basic models); and 3) the hypothesis, which is defined by the rules and variables (also referred to as compound models).

The following sections describe the compound models constructed for the classification of each of the wetland classes together with the associated basic models that build up the compound model in question.

3.3.1 Perennial wetland communities (Compound Model 1)

Wetland communities can be distinguished from other vegetation communities based on their high SWIR absorption, which is due to their relatively higher moisture content. A low moisture stress index value (SWIR/NIR) as well as a high wetness tasselled cap component relative to the surrounding vegetated areas will provide an indication of the existence of wetland communities. The seasonal or perennial nature of these communities will be estimated by means of change vector analysis on the derived vegetation indices and tasselled cap components.

The basic assumption made during the classification of perennial wetland communities was that these communities will remain water saturated throughout the year. This is indicated by a very low amount of change in their moisture stress indices and wetness components when moving from end-of-dry period to end-of-wet period conditions. The high inverse correlation between moisture stress index change and productivity index change means that the same principle can be applied to the change in productivity index. Since water availability is believed to equate to higher productivity, a lower greenness component change can also be expected, adding another principle to perennial wetland classification. The criteria used for the creation of the respective basic models are discussed below.

Basic Model 1: Dry period wetness

Due to the constant water supply to perennial wetland communities, these communities will exhibit a high wetness component even during the dry period. Identifying areas with a high wetness component when compared to surrounding areas at the end of the dry period will identify perennial moisture-rich conditions.

Basic Model 2: Wetness component change (end of wet period to end of dry period)

Change vector analysis on the wetness component between two successive images can be used to estimate the amount and type (increase, decrease, or no change) of change experienced for each pixel. When classifying perennial wetland communities, one would not expect a significant amount of change in the wetness component when moving from end-of-wet period to end-of-dry period conditions, since these wetlands remain saturated throughout the year. Consequently, those pixels experiencing a decrease in their wetness component values when moving from end-of-wet period to end-of-dry period conditions are ruled out of the perennial wetland class.

Basic Model 3: Dry period moisture stress index

Similar to Basic Model 1, constant water supply to perennial wetland communities will cause these communities to exhibit a low moisture stress index value even during the relatively dry growing season. Thresholding the moisture stress index values at the end of the dry period will identify moisture-rich areas, relative to the surrounding vegetation, and will be used as an indication of perennial water availability.

Basic Model 4: Moisture stress index change (end of wet period to end of dry period)

Similar to Basic Model 2, change vector analysis on the moisture stress index between the end-of-wet period and end-of-dry period data sets would provide an indication of the degree of change experienced within those pixels. Here, perennial wetland communities will not exhibit a significant amount of change in moisture stress index value when moving from end-of-wet period to end-of-dry period conditions. Pixels experiencing an increase in moisture stress index (decrease in moisture content) for this time period will be ruled out of the perennial wetland category.

Basic Model 5: Dry period productivity index

Since perennial wetland communities have a constant water supply throughout the annual cycle, water availability during the dry growing season would be associated with higher productivity relative to the surrounding vegetation at the end of the dry period (Viedma *et al.* 1997). Thresholding the productivity index values to identify those areas with a higher productivity compared to the surrounding areas would provide an indication of water availability during the dry period.

Basic Model 6: Productivity index change (end of wet period to end of dry period)

Change vector analysis on the productivity index between the end-of-wet period and end-of-dry period data sets would provide an indication of the degree of change in productivity experienced within those pixels. Due to the high inverse correlation between moisture stress index change and productivity index change (Section 3.2.2.1), one would expect a lesser degree of variability in productivity in perennial wetland communities during an annual cycle.

Basic Model 7: Dry period greenness

Similar to Basic Model 5, water availability during the dry growing season would be associated with higher productivity and, consequently, a higher greenness component compared to the surrounding vegetation. Thresholding the greenness component at the end of

the dry period would identify those areas that are more productive than the surrounding vegetation and, consequently, those areas with a high likelihood of groundwater interaction.

An illustration of the basic models and how they were combined to build up the compound model is illustrated in Figure 3.12. The basic models are combined by a series of AND statements, implying that each of the basic model threshold values must be true in order for a pixel to be classified in the perennial wetland class. The result of the perennial wetland classification is illustrated in Figure 3.13. The output of the perennial wetlands compound model can now be used as input for additional compound models designed for refining the classification of perennial wetlands with a high likelihood of groundwater interaction.

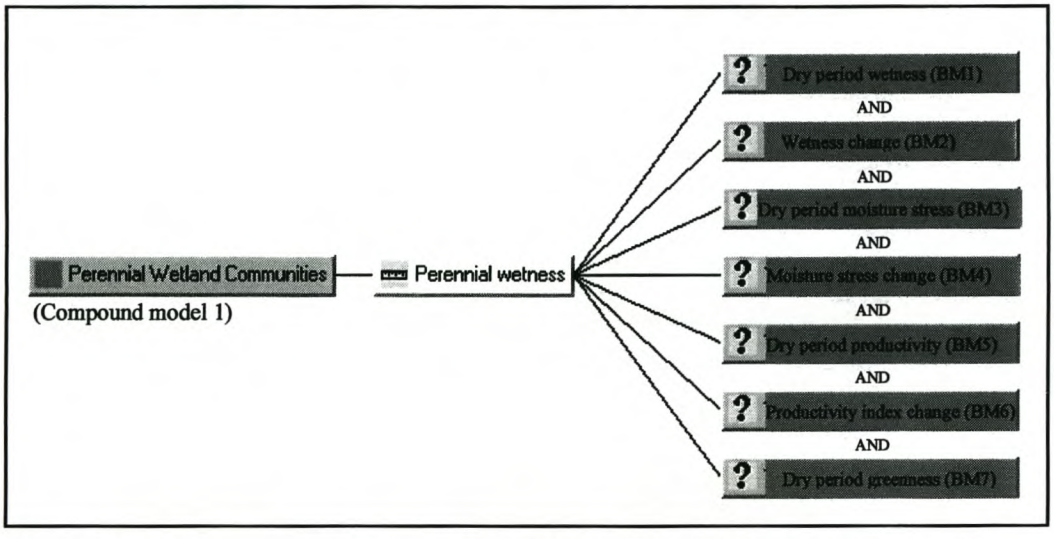

Figure 3.12: Compound model for perennial wetlands classification (BM = Basic Model)

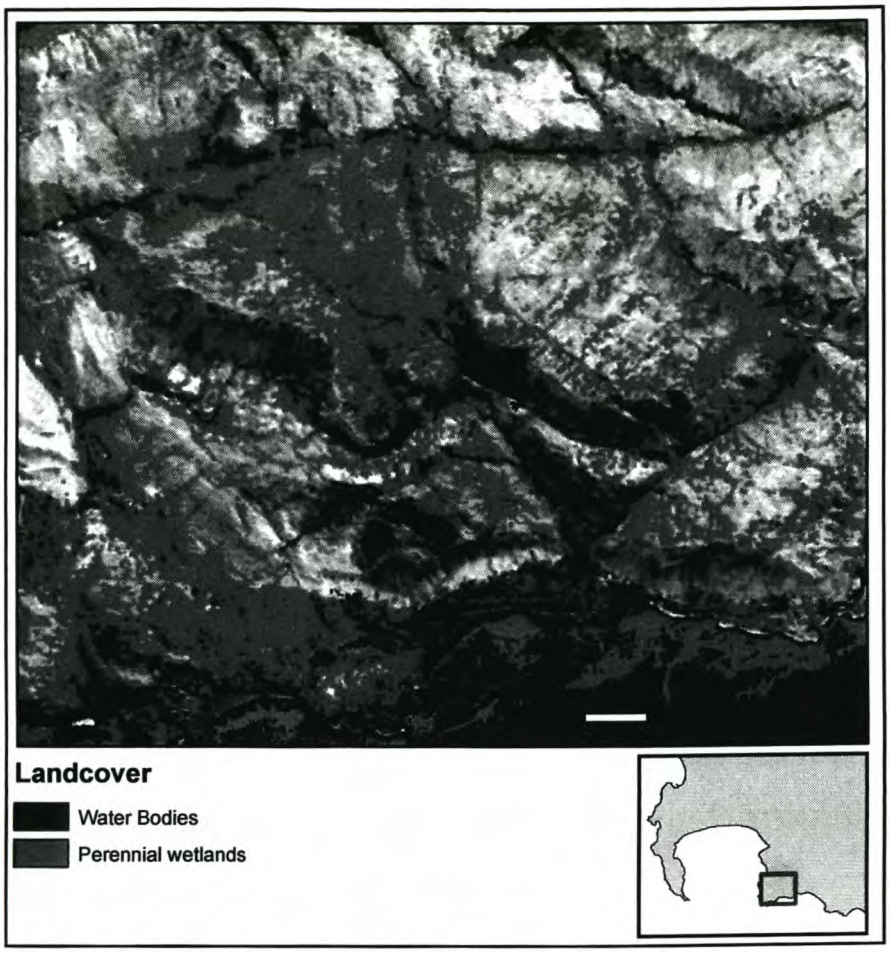

Figure 3.13: Perennial wetlands classification

3.3.2 Perennial wetlands related to geological features (Compound Models 2, 3 and 4)

The output of Compound Model 1 (perennial wetlands) presents the classification of those areas that remain water saturated throughout the annual cycle. Since many of the perennial wetland communities are thought to be dependent on groundwater discharge from the TMG aquifer, it is necessary to identify those wetlands that can be directly associated with geological features that act as water discharge sites. Since the faults in the study area are known to be associated with groundwater discharge (Brown *et al.* 2003), the perennial wetlands situated on these faults are likely to be dependent on groundwater interaction. Additionally, since many of the geological formations are water bearing, the boundaries of these formations are likely sites for aquifer discharge to the surface (Brown *et al.* 2003). For the classification of the geological feature-related wetlands, the output of Compound Model 1 was used as input for Compound Model 2 (fault-related wetlands) as well as Compound Model 3 (lithological boundary-related wetlands). The additional basic models combined with

the output of Compound Model 1 for assessing the proximity to known faults and lithological boundaries are discussed below.

Basic Model 8: Buffer distance to faults

The use of compound model 1, together with a layer identifying those areas within a 70m buffer distance of known faults, resulted in the classification of perennial wetland communities associated with aquifer discharge from faults.

Basic Model 9: Buffer distance to lithological boundaries

The boundaries between the different geological formations were extracted by means of a non-directional edge-detection algorithm. The resulting grid was converted to a vector layer, after which areas within a buffer distance of 70m to the boundaries were extracted. Re-converting the resulting vector layer to grid format provided a suitable lithological boundary layer needed for the construction of this model. The result is a classification of perennial wetland communities situated on the boundaries between the various lithological formations.

Using Basic Models 8 and 9 together with Compound Model 1 will result in an additional wetland category (Compound Model 4), identifying those perennial wetlands occurring in areas where faults and lithological boundaries coincide. These wetlands will have a high probability of groundwater interaction. Similar to Compound Model 1, the basic models are combined by a series of AND statements, implying that each of the basic model threshold values must be true in order for a pixel to be classified in the fault and/or lithological boundary-related wetland class. An illustration of the construction of Compound Model 2, 3 and 4 is illustrated in Figure 3.14 a, b and c respectively.

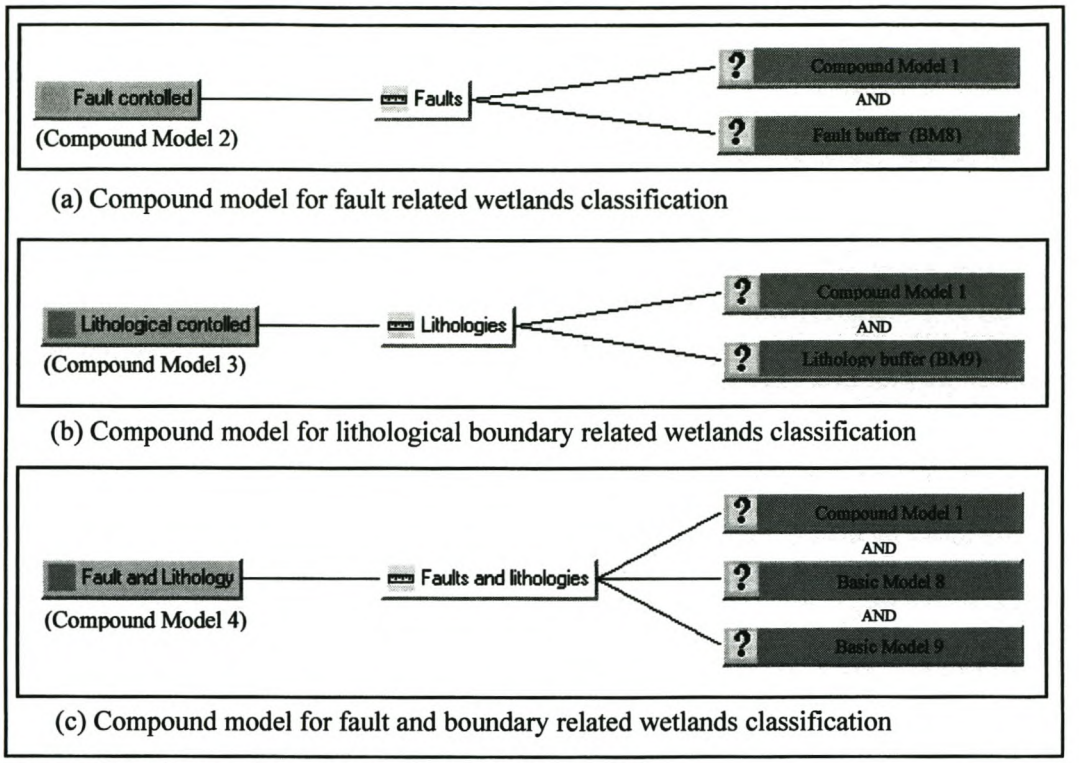

Figure 3.14: Construction of Compound model 2, 3 and 4

The result of the image classification using Compound Models 1 through 4 is illustrated in Figure 3.15.

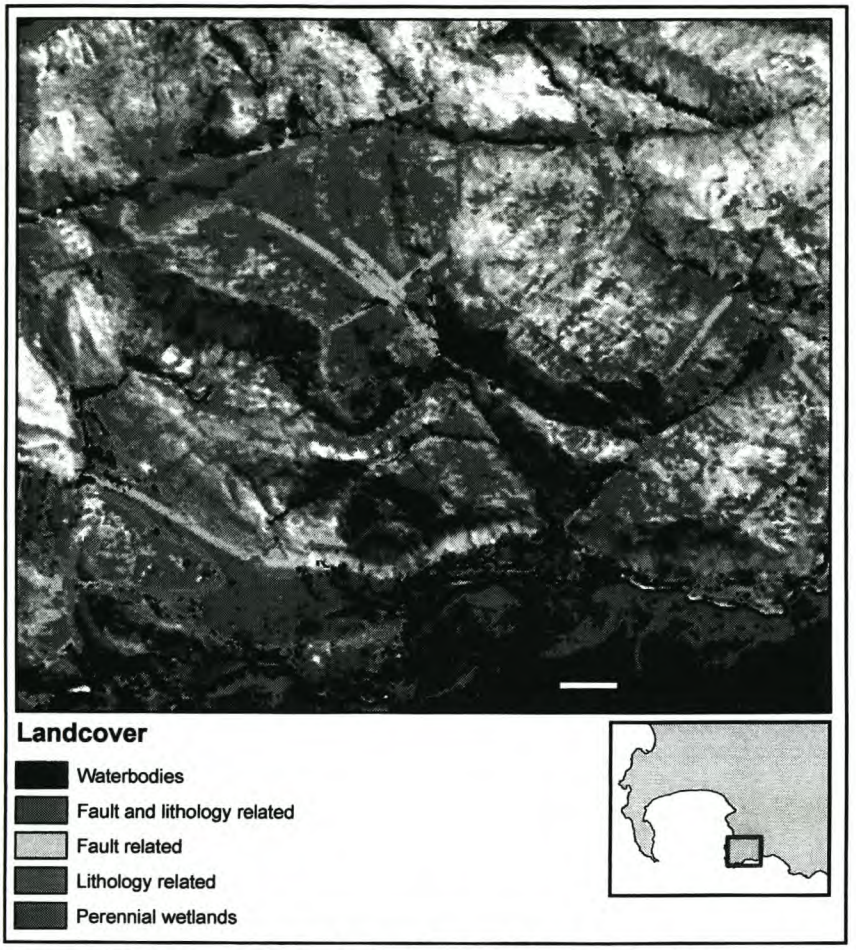

Figure 3.15: Perennial wetland classification discriminating between wetlands occurring on predefined geological conditions

3.3.3 Non perennial groundwater dependent wetlands (Compound Model 5)

The seasonal groundwater dependent wetland communities can be distinguished from their perennial counterparts by analysing the changes they undergo during an annual cycle. Although the non-perennial wetland communities will exhibit the same spectral characteristics as perennial wetlands during the wet season, discontinued water availability during the dry season will cause the seeps to dry up, resulting in a decrease in wetness component and an increase in moisture stress index.

The compound model for the identification of the non-perennial wetland communities was designed to identify those communities with a high likelihood of seasonal groundwater interaction. Additionally, comparing the proximity of these communities to the perennial groundwater-dependent communities could provide an indication of variation in the amount

of groundwater availability during the annual cycle. The basic models employed for the construction of this compound model are discussed below.

Basic Model 10: End of wet period wetness

Defining threshold values for the end-of-wet period wetness components would identify those areas that, during the wet period, are relatively more moisture enriched than their surroundings. Groundwater interaction in these areas will lead to more productive, greener vegetation compared to the surrounding areas, making wetland identification a possibility.

Basic Model 11: Wetness increase (end of dry period to end of wet period)

Non-perennial wetlands would show a significant increase in wetness component when comparing end-of-dry period to end-of-wet period wetness. Identifying these areas will be an indication of wetland communities with only seasonal groundwater interaction.

Basic Model 12: Wetness decrease (end of wet period to end of dry period)

The opposite changes to those described in Basic Model 11 will be experienced by non-perennial wetland communities when moving from end-of-wet period to end-of-dry period conditions. Due to discontinued groundwater contribution to these communities, a decrease in wetness component will be exhibited by these communities, making their identification a possibility.

Basic Model 13: Wet period moisture stress index

Similar to Basic Model 10, thresholding the wet period moisture stress index values could identify those areas with a high amount of healthy green vegetation with higher moisture content than the surrounding areas during the wet period.

Basic Model 14: Moisture stress index increase (end of wet period to end of dry period)

The non-perennial wetland communities are expected to exhibit a large amount of moisture stress during the dry period, while the moisture stress value will be very low during the wet period. Identifying those areas with a significant increase in moisture stress index when moving from end-of-wet period to end-of-dry period conditions would provide an indication of wetland communities with only seasonal groundwater interaction.

Basic Model 15: Moisture stress index decrease (end of dry period to end of wet period)

The opposite conditions to those described in Basic Model 14 will be applicable when comparing end-of-dry period to end-of-wet period moisture stress index values. The non-perennial wetland communities will exhibit a significant decrease in moisture stress when moving from end-of-dry period to end-of-wet period conditions, allowing for the identification of wetland communities with seasonal groundwater interaction.

The combination of basic models used in the construction of this compound model is illustrated in Figure 3.16.

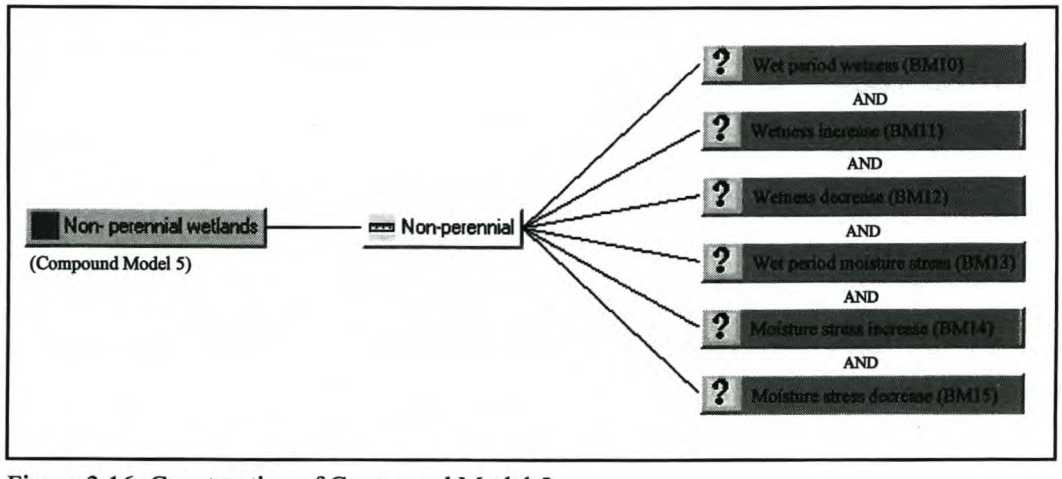

Figure 3.16: Construction of Compound Model 5

3.3.4 Surface flow accumulation (Compound Model 6)

This compound model was designed to classify those wetland communities that form due to surface water accumulation. These communities may have a certain degree of groundwater interaction due to runoff from groundwater discharge sites, but the degree of groundwater interaction in these communities can only be estimated by means of water chemistry studies. Water supply to these communities is mainly due to surface runoff, with water accumulation in topographically suitable areas after precipitation events. Spectrally, these communities are indistinguishable from the non-perennial wetland communities, allowing the use of the output of Compound Model 5 for distinguishing these communities from their perennial counterparts. Additionally, basic models will be added to identify suitable areas for water accumulation. Slopes of less than 8 degrees have been specified as one of the conditions for wetland formation (Kidane 2004). Steeper slopes will result in surface runoff and consequently, wetlands would not have the opportunity to form. Another topographical

parameter that governs the formation of wetland communities is dictated by the curvature of the surface. Suitable curvature conditions, together with gradual slopes, will act as areas where water will accumulate (Arrell 2002), resulting in suitable conditions for wetland formation. The slope and curvature of the landscape were calculated as derivatives of the digital elevation model (DEM) using ArcView 3.3 software. Derivation of curvature of the surface resulted in two output data layers. The first, profile curvature, represents the down-surface shape, while plan curvature represents the cross-surface shape.

Three possible plan curvatures (convex, concave and plane), and three possible profile curvatures (convex, concave and plane) can be distinguished. The variations in plan and profile curves are presented in Figure 3.17.

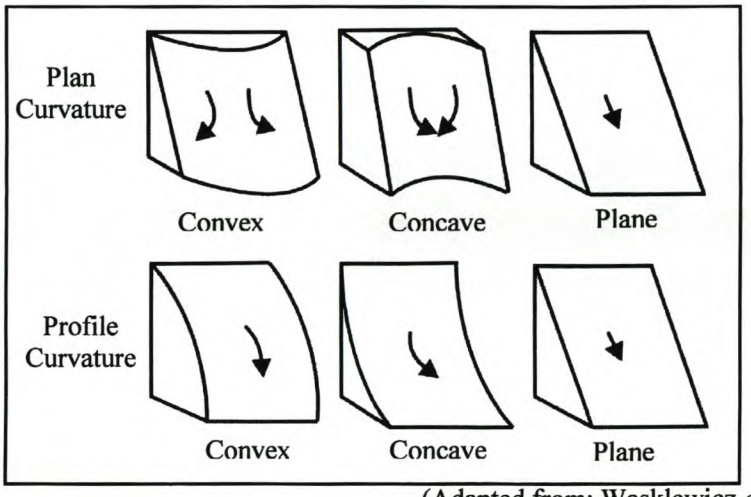

(Adapted from: Wasklewicz *et al.* 2005)

Figure 3.17: Three possible plan- and three possible profile curvatures

If the plan and profile curves are combined, there are nine possible surfaces (refer to Figure 3.18), three of which present suitable areas for water accumulation (Arrell 2002; Wasklewicz, Staley & Seruntine 2005). These are (a) concave-convex areas, (b) concave-concave areas, and (c) planar-concave areas.

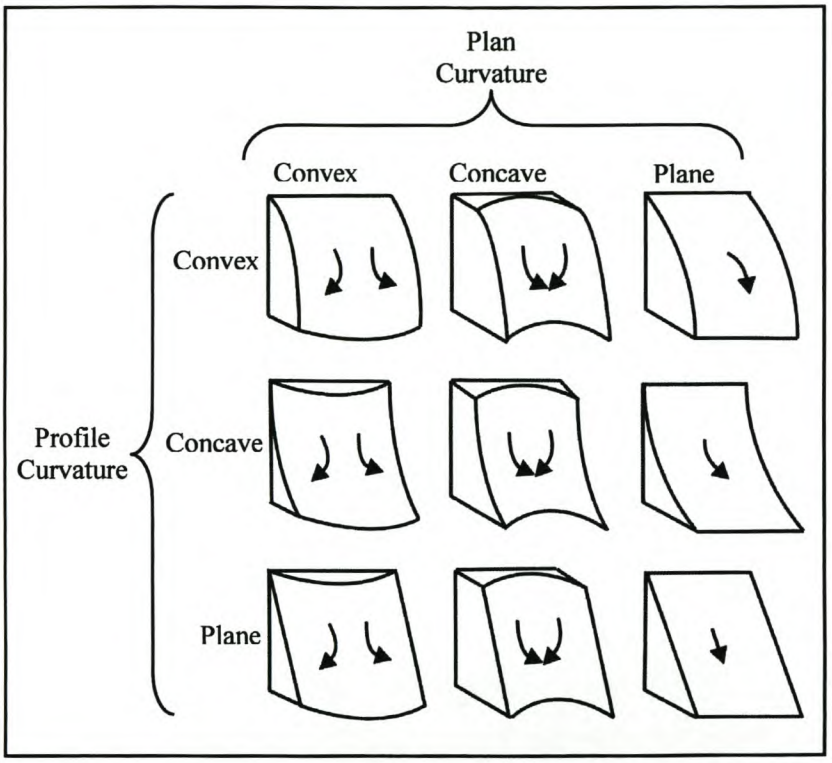

(Adapted from: Wasklewicz *et al.* 2005)

Figure 3.18: Nine possible classes of combined plan and profile curvature

The four additional basic models that will be combined with Compound Model 5 are described below.

Basic Model 16: Slope percentage

According to Kidane (2004), one of the criteria of wetland formation is that gradual slopes must be present. In the presence of steep slopes, surface water will run off until an area is found where water tends to accumulate. Including only those areas with slopes less than 8 degrees in the classification would ensure that only suitable areas are included in the classification.

Basic Model 17: Concave-Convex surface curvature

For both the plan and profile layers the magnitude of the value reflects the degree of curvature, while the sign reflects the convexity or concavity of the surface (Wasklewicz *et al.* 2005). Concave curvatures are presented with negative numbers, planar surfaces with a zero, and convex curvatures with positive numbers. Specifying negative numbers for plan curvature

and positive numbers for the profile curvature data layers will result in the inclusion of areas with a combined concave-convex curvature and, consequently, those areas where water is likely to accumulate.

Basic Model 18: Concave-Concave surface curvature

Similar to Basic Model 17, the specification of negative numbers for both plan and profile curvatures will result in the inclusion of concave-concave curvatures, another likely area for surface water accumulation.

Basic Model 19: Planar-Concave surface curvature

Specifying a zero value for the plan curvature layer combined with negative numbers for the profile curvature layer will ensure the inclusion of a combined planar-concave curvature.

The compound model constructed for the identification of wetlands formed due to surface water accumulation is presented in Figure 3.19. The final wetland classification map is presented in Figure 3.20.

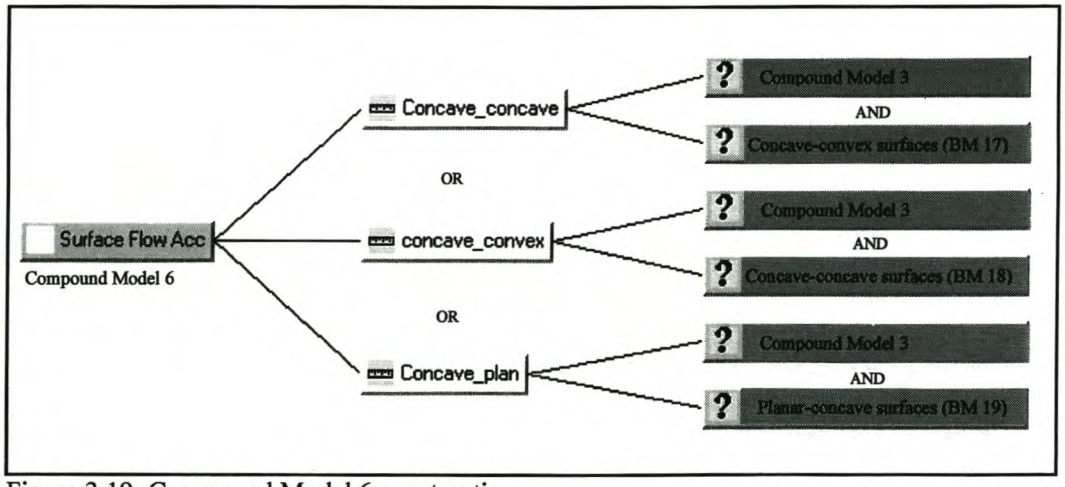

Figure 3.19: Compound Model 6 construction

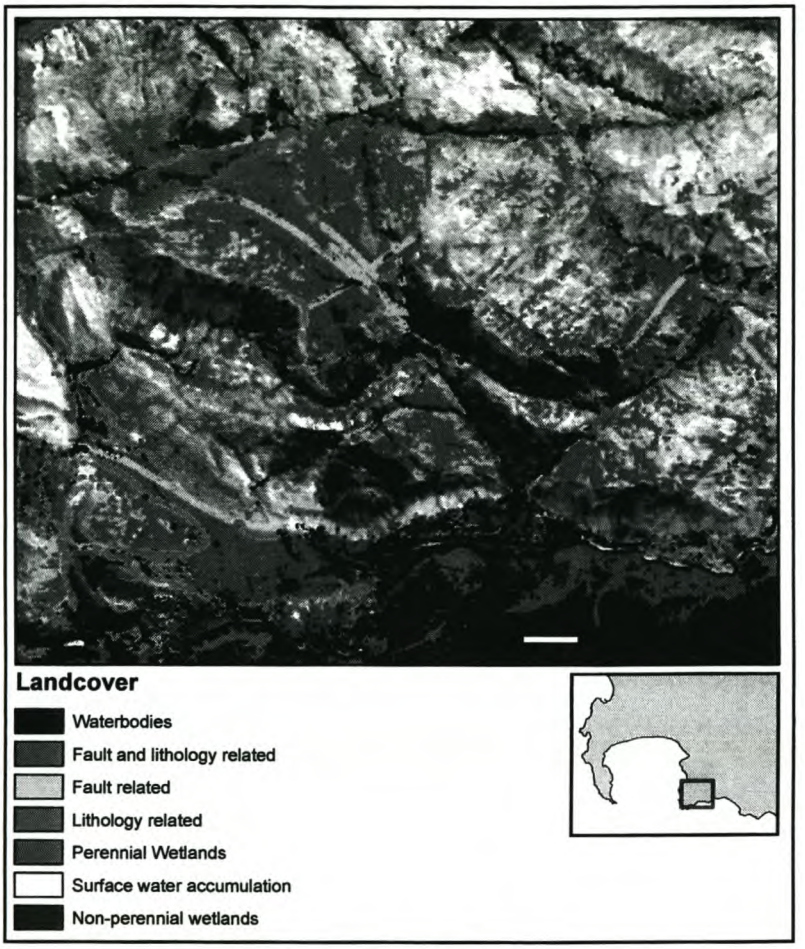

Figure 3.20: Final wetlands classification map

3.4 ASSESSMENT OF CLASSIFICATION ACCURACIES

According to Lillesand, Kiefer & Chipman (2004), no classification is complete until the accuracy of the classification has been assessed. Accuracy assessment is usually achieved by constructing an error matrix in which the relationship between reference data and the result of image classification can be presented. This error matrix is constructed by listing the known cover types used for training versus the pixels actually classified into each landcover category (Lillesand *et al.* 2004). However, since the ground truth data representing the GPS coordinates of known wetland communities does not include detail about the nature of the wetland communities, or a sufficient description of the geological or topographic conditions associated with the observed communities, the error matrix method could not be used. Consequently, only the perennial wetlands class was inspected for accuracy assessment purposes. Accuracy assessment was performed by determining the percentage of pixels in the

reference data set that were correctly classified as perennial wetlands. The percentage of correctly classified training pixels was also estimated. The result is presented in Table 3.4.

Table 3.4: Quantifying the accuracy of the perennial wetlands classification process

	Training Pixels	Reference Pixels
Basic Model 1	98.41%	92.06 %
Basic Model 2	98.41 %	87.30 %
Basic Model 3	96.83 %	87.30 %
Basic Model 4	93.65 %	77.78 %
Basic Model 5	93.65 %	77.78 %
Basic Model 6	90.48 %	77.78 %
Basic Model 7	90.48 %	77.78 %
Total number of Pixels	63	63
Total Accuracy (%)	90.48%	77.78%

This table represents the cumulative producer's accuracy of the perennial wetlands classification after each basic model has been added. For example, for the training data, the accuracy after Basic Models 1 and 2 is 98.41%, but after Basic Model 3 is added, the accuracy decreases to 96.83%. The total accuracy of training pixel classification is 90.48% while the reference pixels were classified at a total accuracy of 77.78%. In order to fully assess the accuracy with which a particular feature or class is identified, information regarding the presence as well as the absence of the feature needs to be considered. Therefore areas where the feature occurs, as well as areas where the feature does not occur, is needed. The result of the accuracy assessment done during this study is misleading since only areas were wetlands communities are present were used during accuracy quantification. Consequently, if the entire image were classified as wetlands, the producer's accuracy would have been 100%, which is obviously not accurate.

Errors of omission describe the number of pixels that should have been classified as perennial wetlands, but were omitted from this class. From Table 3.4 one can gather that fewer pixels that should have been classified as perennial wetlands are classified as such with the addition of each basic model, implying that the error of omission increases. Errors of commission, on the other hand, describe the number of pixels that were classified as perennial wetlands, but in reality belong to a different class altogether. The lack of data pertaining to non-wetland

vegetation classes means that errors of commission could not be quantified. However, visual inspection of Figure 3.21 reveals that the total number of classified pixels decrease with the addition of each basic model. It could be therefore be expected that, together with the number of pixels that were correctly classified, the number of pixels that were wrongly classified as perennial wetlands would also decrease, resulting in a subsequent decrease in errors of commission. In order to verify the decrease in errors of commission, however, detailed ground truth data are required.

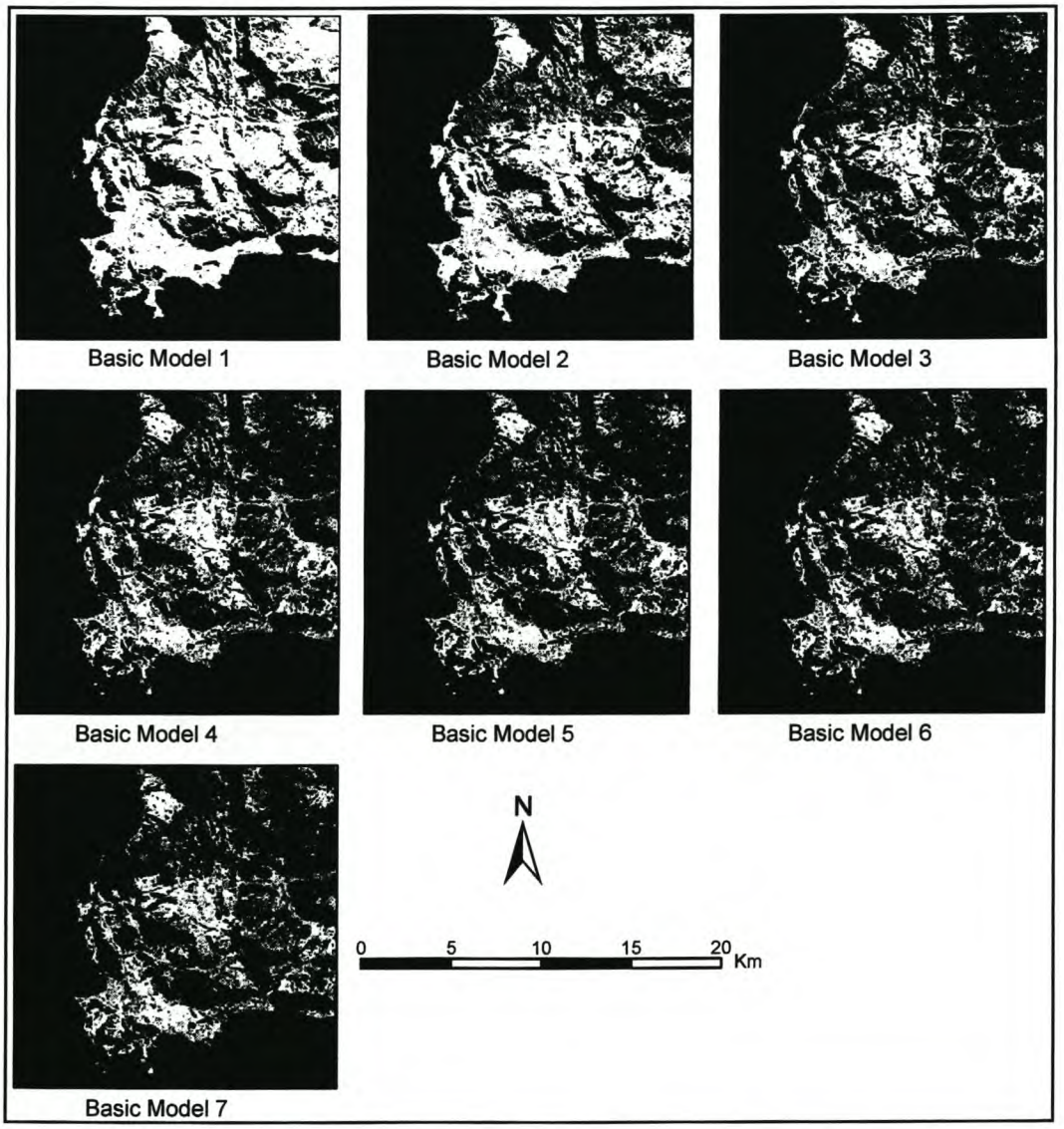

Figure 3.21: Output of classification process after each basic model addition (White = Perennial wetlands, Black = Undefined)

CHAPTER 4: DISCUSSION AND RECOMMENDATIONS

4.1 DISCUSSION OF THE RESULTS

The main objective of the study was to establish whether Landsat 7 data could be used for the identification of groundwater-dependent ecosystems. This ability was demonstrated with a high level of accuracy by using a combination of tasseled cap components and vegetation indices to identify the existence of wetland vegetation. The success of change vector analysis using tasseled cap components and vegetation indices demonstrated the technique's ability to estimate the seasonal changes experienced in the wetland communities, and consequently provide an estimate to the degree of groundwater dependency.

While change vector analysis can be used to detect a variety of changes, this study was only concerned with change related to different degrees of groundwater interaction. In the case of perennial groundwater dependency, a low degree of changes is expected during an annual cycle. The perennial groundwater-dependent ecosystems will remain consistently moisture enriched (low degree of change in wetness component and moisture stress index) and, consequently, consistently productive (low degree of change in productivity index). When these change detection strategies are applied in a monitoring exercise, significant changes experienced in known wetland communities may reveal unnatural fluctuations in groundwater availability to these communities, and the necessary corrective steps can be taken. In the case of non-perennial wetlands, significant changes in moisture stress index and wetness component are expected during the annual cycle. The proximity of these communities to perennial groundwater-dependent communities may be an indication of wetland expansion due to additional water availability from precipitation during the wet period.

The absence of wetlands on the south facing slopes is misleading. Their absence is due to the presence of shadows on the 18 May 2002 image. Since spectral responses of landcover classes can not be extracted from areas covered by shadows, these areas were masked out of the classification procedure. An astonishing amount of perennial wetlands were classified on the final landcover map. It is unlikely that such a large amount of perennial wetland communities are indeed present. This is an indication that classification threshold values need adjustment. This would however result in diminished classification accuracy. From the classification accuracy assessment, one could infer that when classifying the wetland communities, there would be a trade-off between errors of omission and errors of

commission. The use for which the output of the image classification procedure will be applied would dictate a suitable mid-way between these errors. If the output will be used solely for the monitoring of the changes experienced in known perennial wetland communities, larger errors of commission might be overlooked. However, if the classification procedure is aimed at identifying wetland communities with a high likelihood of groundwater interaction, errors of commission should be kept to a minimum. Future studies should concentrate on reducing both the errors of omission and the errors of commission in order to produce a system that can be utilized for addressing both problems. The following section will consist of the researcher's recommendations for increasing the classification accuracies. Possible follow-up studies on remote sensing for monitoring groundwater-dependent ecosystems are also recommended.

4.2 RECOMMENDATIONS FOR FUTURE RESEARCH

4.2.1 Increasing classification accuracies

Further studies on the classification of groundwater-dependent wetland communities should concentrate on increasing the accuracy of the classification. Possible reasons for insufficient classification accuracy in this study that can be addressed during subsequent research are indicated below.

- *Lack of topographic normalisation and the impact on tasselled cap components*: According to Lu, Mausel, Brondízio & Moran (2004) the brightness and greenness components of the tasselled cap transformation is highly sensitive to topographic variation within a scene. Due to software constraints, the topographic normalisation was not performed, but performing this normalisation to correct for the bi-directional reflectance effect will alleviate this sensitivity to topographic variation, with the added possibility of significantly enhancing the classification results.
- *Cloud formations on imagery and masking of cloud shadows*: The 23 September 2002 image is influenced by a significant presence of clouds over the area. Although atmospheric correction effectively masked out the optically thick cloud layers, spectral data beneath these cloud regions could not be extracted, and hence change detection in these regions could not be performed. Additionally, the shadows cast by the cloud formations constitute additional areas for which pixel data could not be extracted, meaning that large areas of this image could not be used in the change detection process. Using cloud-free data will improve change detection strategies and classification results.

- *Problems related to thresholds for the identification of vegetation classes*: Classification of wetland communities was performed by thresholding the change vector data in order to create images indicating positive, negative and no-change vectors. However, according to Wilson, Nelson, Boots & Wulder (2004), threshold selection is generally the most subjective and most problematic step in the change detection process. Allen & Kupfer (2000) defined thresholds using statistical analysis in a local measure of auto-correlation, which allows for the identification of clusters of similar change that are extreme relative to the mean change. Using this method for the estimation of threshold values should be considered for improving classification results.
- *Nominal frequency of remote sensor data acquisitions*: According to Lunetta *et al.* (2004), an important consideration for monitoring landcover change is the temporal frequency of data acquisitions required to characterise change events adequately. According to Rogan *et al.* (2002), errors found in vegetation change detection can be a result of sizable differences in precipitation during the time of the study. They found that inter-annual phonological variability caused by variable precipitation patterns can produce errors in identifying temporal changes. The researcher suggests that annual changes in vegetation productivity be analysed in conjunction with precipitation data in order to estimate changes in productivity in relation to changes in precipitation.
- *Lack of sufficient ground truth data and detailed field work:* An in-depth groundtruthing exercise including an assessment of the degree of groundwater dependency is necessary for the identification of satisfactory training sites for the classification of the different types of wetland communities, as well as for the proper assessment of classification accuracy.

4.2.2 Follow-up studies on remote sensing for groundwater dependent ecosystems

In order to estimate the viability of using remote sensing data for monitoring the ecosystems in question, an in-depth study of alternative satellite sensors that could be used should be conducted. According to Colvin *et al.* (2002), the suitability assessment should include the following:

a) Availability, addressing the issue of whether satellite imagery of the study area is available and if routine image acquisitions are a possibility. Continuity is also important, especially where the project is focused on monitoring. There must be

certainty that the satellite will not be decommissioned or that the series will not be discontinued;

b) Spectral characteristics of the sensor should be investigated to determine if the bands most common for vegetation studies (visible, near infrared and shortwave infrared) are present;
c) Spatial resolution should be considered because the size of the wetland communities under investigation would influence the choice of satellite sensor;
d) Cost, the most limiting factor, can be assessed in terms of a cost-benefit analysis, describing the cost implications for using the remote sensing data for monitoring of wetland communities instead of by fieldwork.

Some alternative sensors to the multispectral imagery (such as Landsat) should be investigated in terms of addressing the vegetation-related questions. Alternative sensors include hyperspectral sensors (Asner, Wessman, Bateson & Privette 2000; Short 2003; Zhang *et al.* 2003), very high-resolution sensors (Hirose, Mori, Akamatsu & Li 2003; Narsavage, Gentry & Weber 2004) and radar remote sensors (Moran, Hymer, Qi & Kerra Y 2002; Wang, Qi, Moran & Marsett 2004).

Irrespective of the satellite sensor used, studies are needed which focus on addressing questions such as:

- Where are the different groundwater-dependent ecosystems situated and what are their size?
- Does the size of these communities change during an annual cycle?
- How are these communities influenced by climate changes such as precipitation fluctuations?
- Which satellite sensors could be used as alternatives, but would still provide comparable results?

Campbell (1996) states that human activities are rapidly destroying large areas of ecological importance and that the multi-temporal availability of remote sensing data may provide the only practical means of mapping and monitoring the changes in these areas. The various image processing and classification techniques should be applied to a time-series of images over a large number of years in order to estimate the normal growing conditions and mean changes experienced in the wetland communities during an annual cycle. Characterising the health and moisture content of wetlands relative to this norm will provide the capability of

estimating where deviations from the expected seasonal patterns are occurring. These deviations will be an indication of external factors influencing plant growth. Monitoring of the wetland ecosystems performance could lead to the early detection of vegetation degradation as a result of discontinued water availability and the necessary corrective steps could then be taken.

REFERENCES

Allen, TR & Kupfer JA, 2000. Application of spherical statistics to change vector analysis of Landsat data: Southern Appalachian spruce-fir forests. *Remote Sensing of Environment* 74: 482–493.

Arrell KE 2002. Geographical Information Systems (GIS): A useful tool for Geomorphologists? Journal of the Durham University Geographical Society http://www.geog.leeds.ac.uk/people/k.arrell/GeomorphologyAndGIS.pdf. [Accessed March 2005].

Asner GP, Wessman CA, Bateson CA & Privettes JL 2000. Impact of tissue, canopy and landscape factors on the hyperspectral reflectance variability of arid ecosystems. *Remote sensing of the environment* 74: 69-84.

Boucher C 1982. The Kogelberg state forest and environs: a paradise for Cape Flora. *Veld & Flora* 68, 1: 8-11.

Brown C, Colvin C, Hartnady C, Hay R, Le Maitre D & Riemann K, 2003. Ecological and environmental impacts of large-scale groundwater development in the Table Mountain Group (TMG) aquifer system. Discussion paper for scoping phase. WRC project K5/1327.

Budde ME, Tappan G, Rowland J, Lewis J & Tieszen L 2004. Assessing land cover performance in Senegal, West Africa using 1-km integrated NDVI and local variance analysis. *Journal of Arid Environments* 59, 3: 481-498.

Campbell JB 1996. *Introduction to remote sensing, 2nd Edition.* London: Taylor & Francis Ltd.

Ceccato P, Flasse S, Tarantola S, Jacquemoud S & Grégoire J-M 2001. Detecting vegetation leaf water content using reflectance in the optical domain. *Remote Sensing of Environment,* 77, 1: 22-33.

Chavez PS 1988. An improved dark-object subtraction technique for atmospheric scattering correction of multispectral data. *Remote Sensing of Environment* 24: 459-479.

Collado AD, Chuvieco E & Camarasa A 2002. Satellite remote sensing analysis to monitor desertification processes in the crop-rangeland boundary of Argentina. *Journal of Arid Environments* 52, 1: 121-133.

Collins JB & Woodcock CE 1996. An assessment of several linear change detection techniques for mapping forest mortality using multitemporal Landsat TM data. *Remote Sensing of Environment* 56, 1: 66-77.

Colvin C, Le Maitre D & Hughes S 2002. Assessing terrestrial groundwater dependent ecosystems is South Africa. WRC project.

Coppin P 2002. Physical principles of the remote sensing of dynamic processes. Course notes presented by the Faculty of Agricultural and Forestry Sciences and the Department of Electronic Engineering, University of Stellenbosch.

Doraiswamy PC, Hatfield JL, Jackson TJ, Akhmedov B, Prueger J & Stern A 2004. Crop condition and yield simulations using Landsat and MODIS. *Remote Sensing of Environment* 92, 4: 548-559.

Environmental Potential Atlas (ENPAT) 2001. Cape Hangklip Geology. (Map).

French AN, Schmugge TJ and Kustas WP 2000. Discrimination of senescent vegetation using thermal emissivity contrast. *Remote Sensing of Environment* 74: 249-254.

Gitelson AA, Kaufman YJ & Merzlyak MN 1996. Use of a green channel in remote sensing of global vegetation from EOS- MODIS. *Remote Sensing of Environment 58,* 3: 289-298.

Hartnady CJH, Jackson C & Riemann K 2004. Hydrogeological selection process report. Report Number.

Hatfield PL & Pinter PJ 1993. Remote sensing for crop protection. *Crop Protection* 12, 6: 403-413.

Hirose Y, Mori M, Akamatsu Y & Li Y 2003. Vegetation cover mapping using hybrid analysis of IKONOS data [online]. Available from http://www.isprs.org/istanbul2004/comm7/papers/56.pdf. [Accessed 1 September 2004]

Huang C, Yang L, Homer C, Wylie B, Vogelman J & DeFelice T 2001. *At satellite reflectance: A first order normalization of Landsat 7 ETM + images* [online]. Available from http://landcover.usgs.gov/pdf/huang2.pdf. [Accessed 1 September 2004].

Irish RR 2000. *Landsat 7 Science data user's handbook; Report 430-15-01-003-0, National Aeronautics and Space Administration* [online]. Available from http://bsrsi.msu.edu/trfic/data_portal/Landsat7doc/toclandsat. [Accessed 5 June 2004].

Kidane DK 2004. Rule-based land cover classification model: Expert system integration of image and non-image spatial data. MSc-thesis. Stellenbosch: University of Stellenbosch (Department of Geography and Environmental Studies).

Lelong CCD, Pinet PC & Poilvé H 1998. Hyperspecral imaging and stress mapping in agriculture: A case study on wheat in Beauce (France). *Remote Sensing of Environment* 66, 2: 179-191.

Levien LM, Fischer CS, Roffers PD & Maurizi BA 1998. *Statewide change detection using multitemporal remote sensing data* [online]. Available from http://frap.cdf.ca.gov/projects/change_detection/pdfs/erim.pdf. [Accessed 17 October 2004].

Lillesand TM, Kiefer RW & Chipman JW 2004. *Remote sensing and image interpretation.* 5th ed. New York: Wiley & Sons, Inc.

Lorena RB, dos Santos JR, Shimabukuro YE, Brown IF & Kux HJH 2002. *A change vector analysis technique to monitor land use/land cover in SW Brazillian Amazon: Acre state* [online]. Available from http://www.isprs.org/commission1/proceedings/paper/00014.pdf. [Accessed 6 June 2004].

LP DAAC staff 2004. *Landsat-7 Level-0 and Level-1 Data Sets Document* [online]. Available from http://eosims.cr.usgs.gov:5725/DATASET_DOCS/landsat7_dataset.html. [Accessed 26 June 2004].

Lu D, Mausel P, Brondízio E & Moran E 2004. Relationships between forest stand parameters and Landsat TM spectral responses in the Brazilian Amazon Basin. *Forest Ecology and Management,* 198, 1-3: 149-167.

Lück W 2004. Remote Sensing: A powerful but labour intensive tool for precision forestry. How can information extraction be automated? Precision Forestry Workshop, Pietermaritzburg, 22-23 June.

Lunetta RS, Johnson DM, Lyon JG & Crotwell J 2004. Impacts of imagery temporal frequency on land-cover change detection monitoring. *Remote Sensing of Environment* 89, 4: 444-454.

Mbow C, Goïta K, Bénié GB 2004. Spectral indices and fire bahaviour simulation for fire risk assessment in savanna ecosystems. *Remote Sensing of Environment* 9, 1: 1-13.

Moran MS, Hymer DC, Qi J, & Kerra Y 2002. Comparison of ERS-2 SAR and Landsat TM imagery for monitoring agricultural crop and soil conditions. *Remote Sensing of Environment* 79: 243-252.

Moran MS, Clarke TR, Inoue Y & Vidal A 1994. Estimating crop water deficit using the relation between surface-air temperature and spectral vegetation index. *Remote Sensing of Environment* 49, 3: 246-263.

Munyati C 2000. Wetland change detection on the Kafue Flats, Zambia, by classification of a multitemporal remote sensing image dataset. *International Journal Remote Sensing* 21, 9: 1787-1806.

Narsavage D, Gentry C & Weber KT 2003. White paper report: a comparison of NDVI models generated using Quickbird and Landsat 7 ETM+ data [online]. Available from http://giscenter.isu.edu/research/techpg/blm_fire/NDVI_Report.pdf. [Accessed 1 September 2004]

Ninham Shands. 2004. TMG Aquifer Feasibility Study and Pilot Project: Draft Scoping Report. Report Number 400396/3715.

Pani D 2001. A Simple Image Enhancement Procedure for an EROS Scene of the Tresnuraghes Area (Sardinia, Italy) [online]. Available from http://www.imagesatintl.com/usesapplications/casestudies/EROSTresnuraghes.pdf. [Accessed 13 October 2004].

Parker DC & Wolff MF, 1965. Remote Sensing. International Science and Technology 43:20-31.

Patterson MW & Yool SR 1998. Mapping fire-induced vegetation mortality using Landsat Thematic Mapper data: a comparison of linear transformation techniques. *Remote Sensing of Environment* 65, 2: 132-142.

PCI 2003. PCI Geomatica V9.1. PCI Geomatics Enterprises Inc.

Pradhan S 2001. Crop area estimation using GIS, remote sensing and area frame sampling. *International Journal of Applied Earth Observation and Geoinformation* 3, 1: 86-92.

Rogan J, Franklin J & Roberts DA 2002. A comparison of methods for monitoring multitemporal vegetation change using Thematic Mapper imagery. *Remote Sensing of Environment* 80, 1: 143-156.

Shao Y, Fan X, Liu H, Xiao J, Ross S, Brisco B, Brown R & Staples G 2001. Rice monitoring and production estimation using multitemporal RADARSAT. *Remote Sensing of Environment* 76, 3: 310-325.

Short NM 2003. *Vegetation applications: Agriculture, forestry and ecology* [online]. Available from http://rst.gsfc.nasa.gov/Sect3/Sect3_1.html. Accessed [3 June 2004].

Sims DA & Gamon JA 2003. Estimation of vegetation water content and photosynthetic tissue area from spectral reflectance: a comparison of indices based on liquid water and chlorophyll absorption features. *Remote Sensing of Environment* 84: 526- 537.

Skakun RS, Wulder MA & Franklin SE 2003. Sensitivity of the thematic mapper enhanced wetness difference index to detect mountain pine beetle red-attack damage. *Remote Sensing of Environment* 86, 4: 433-443.

Song C, Woodcock CE, Seto KC, Lenney MP & Macomber SA 2001. Classification and change detection using Landsat TM data: When and how to correct atmospheric effects? *Remote Sensing of Environment* 75, 2: 230-244.

Theron JN, Gresse PG, Siegfried HP & Rogers J 1992. *The geology of the Cape Town area.* Department of Mineral and Energy Affairs, Pretoria.

Tottrup C & Rasmussen MS 2004. Mapping long-term changes in savanna crop productivity in Senegal through trend analysis of time-series of remote sensing data. *Agriculture, Ecosystems & Environment* 103, 3: 545-560.

USGS 2001. *MRLC 2001 Image preprocessing procedure* [online]. Available from http://landcover.usgs.gov/pdf/image_preprocessing.pdf. [Accessed 1 September 2004].

Urban DL 2000. *Multivariate analysis in ecology: Multivariate ecological dynamics* [online]. Available from http://www.env.duke.edu/lel/env358/mv_cva.pdf. [Accessed 11 June 2004].

Vergara OR s.d. Pre-processing of orbital images at INPE [online]. Available from http://www.photogrammetry.ethz.ch/general/persons/jana/isprs/tutmapup/ISPRS_tutorial_preprocessing.pdf. [Accessed September 2004]

Viedma O, Meliá J, Segarra D & Garcia-Haro J 1997. Modeling rates of ecosystems recovery after fires by using Landsat TM data. *Remote Sensing of Environment* 61, 3: 383-398.

Wang C, Qi J, Moran S & Marsett R 2004. Soil moisture estimation in semi-arid rangeland using ERS-2 and TM imagery. *Remote Sensing of Environment* 90: 178-189.

Wasklewicz T, Staley M & Seruntine L 2005. Recording lichen species in Shenandoah National Perk using terrestrial 3D laser scanning techniques [online]. Available from http://geography.memphis.edu/thad/nsf/articles/SNP_Laser.pdf. [Accessed 25 April 2005].

Weier J & Herring D 2001. Measuring vegetation (NDVI & EVI) [online]. Available from http://earthobservatory.nasa.gov/Library/MeasuringVegetation. [Accessed 16 September 2004].

Western Cape Nature Conservation Board, Scientific Services 2000. *Kogelberg vegetation.* (Map). Cape Town: Environmentek CSIR.

Wilson HG, Nelson T, Boots B & Wulder MA 2004. Using a spatial statistic threshold technique for defining change in a forested environment [online]. Available from http://www.casi.ca/papers/3-19.pdf. Accessed February 2005.

Xiaoliang W, Danaher T, Wallace J & Campbell N 2001. A Landsat 7 calibration base for Australia [online]. Available from http://www1.cmis.csiro.au/RSM/research/pdf/Wu_SPIE2001.pdf. [Accessed September 2004]

Zhang Y 2004. Understanding image fusion. *Photogrammetric Engineering and Remote Sensing* 657-661.

Zhang Q, Pavlic G, Chen W, Latifovic R, Fraser R & Cihlar J 2004. Deriving stand age distribution in boreal forests using SPOT VEGETATION and NOAA AVHRR imagery. *Remote Sensing of Environment* 91, 3-4: 405-418.

Zhang M, Qin Z, Liu X & Ustin SL 2003. Detection of stress in tomatoes induced by late blight disease in California, USA, using hyperspectral remote sensing. *International Journal of Applied Earth Observation and Geoinformation* 4, 4: 295-310.